

Group Spike and Slab Variational Bayes

Michael Komodromos*, Kolyan Ray, Marina Evangelou and Sarah Filippi
Department of Mathematics, Imperial College London

September 20, 2023

Abstract

In this manuscript we introduce Group Spike-and-slab Variational Bayes (GSVB), a scalable method for group sparse regression. We construct a fast co-ordinate ascent variational inference algorithm for several model families including: the Gaussian, Binomial and Poisson. Through extensive numerical studies we demonstrate that GSVB provides state-of-the-art performance, offering a computationally inexpensive substitute to MCMC, whilst performing comparably or better than existing MAP methods. Additionally, we analyze three real world datasets wherein we highlight the practical utility of our method, demonstrating that GSVB provides parsimonious models with excellent predictive performance, variable selection and uncertainty quantification.

*M.K. gratefully acknowledge EPSRC's StatML CDT, Imperial's CRUK center and Imperial's Experimental Cancer Medicine center.

1 Introduction

Group structures arise in various applications, such as genetics (Wang et al., 2007; Breheny and Huang, 2009), imaging (Lee and Cao, 2021), multi-factor analysis of variance (Meier et al., 2008), non-parametric regression Huang et al. (2010), and multi-task learning, among others. In these settings, p -dimensional feature vectors, $x_i = (x_{i1}, \dots, x_{ip})^\top \in \mathbb{R}^p$, for $i = 1, \dots, n$ observations can be partitioned into groups of features. Formally this means, we can construct sub-vectors, $x_{G_k} = \{x_j : j \in G_k\}$ for $k = 1, \dots, M$, where the groups $G_k = \{G_{k,1}, \dots, G_{k,m_k}\}$ are disjoint sets of indices satisfying $\bigcup_{k=1}^M G_k = \{1, \dots, p\}$. Typically, these group structures are known beforehand, for example in genetics where biological pathways of gene sets are known, or they are constructed artificially, for example, through a basis expansion in non-parametric additive models.

In the regression setting incorporating these group structures is crucial, as disregarding them can result in sub-optimal models (Huang and Zhang, 2010; Lounici et al., 2011). One method of doing so, which we focus on in this manuscript, is via general linear regression. Under this framework the response, Y_i , for each observation $i = 1, \dots, n$, can be modelled by,

$$\mathbb{E}[Y_i|x_i, \beta] = f\left(\sum_{k=1}^M x_{i,G_k}^\top \beta_{G_k}\right), \quad i = 1, \dots, n \quad (1)$$

where $f : \mathbb{R} \rightarrow \mathbb{R}$ represents the link function, $\beta = (\beta_1, \dots, \beta_p)^\top \in \mathbb{R}^p$ denotes the model coefficient vector with $\beta_{G_k} = \{\beta_j : j \in G_k\}$.

Beyond incorporating the group structure, it is often of practical importance to identify the groups of features that are associated with the response. This holds particularly true when there are a large number of them. To address this, various methods have been proposed over the years, with one of the most popular being the group LASSO (Yuan and Lin, 2006), which applies an $\ell_{2,1}$ norm to groups of coefficients. Following Yuan and Lin (2006) there have been numerous extensions, including the group SCAD (Wang et al., 2007), the group LASSO for logistic regression (Meier et al., 2008), the group bridge (Huang et al., 2009), group LASSO with overlapping groups (Jacob et al., 2009), and the sparse group LASSO (Breheny and Huang, 2009; Simon et al., 2013), among others (see Huang et al. (2012) for a detailed review of frequentist methods).

In a similar vein, Bayesian group selection methods have arisen. The earliest of which being the Bayesian group LASSO (Raman et al., 2009; Kyung et al., 2010), which uses a

multivariate double exponential distribution prior to impose shrinkage on groups of coefficients. Notably, the maximum a posteriori (MAP) estimate under this prior coincides with the estimate under the group LASSO. Other methods include Bayesian sparse group selection (Xu and Ghosh, 2015; Chen et al., 2016) and the group spike-and-slab LASSO (Bai et al., 2020) which approach the problem via stochastic search variable selection (Mitchell and Beauchamp, 1988; Chipman, 1996). Formally, these methods utilize a group spike-and-slab prior, a mixture distribution of a multivariate Dirac mass on zero and a continuous distribution over \mathbb{R}^{m_k} , where m_k is the size of the k th group. Such priors have been shown to work excellently for variable selection as they are able to set coefficients exactly to zero, avoiding the use of shrinkage to enforce sparsity. For a comprehensive review see Lai and Chen (2021) and Jreich et al. (2022).

However, a serious drawback of these methods is that most use Markov Chain Monte Carlo (MCMC) to sample from the posterior (Raman et al., 2009; Xu and Ghosh, 2015; Chen et al., 2016). In general, MCMC approaches are known to be computationally expensive when there are a large number of variables, and within the group setting they can result in poor mixing when group sizes are large (Chen et al., 2016). To circumvent these issues, some authors proposed computing MAP estimates (Kyung et al., 2010; Bai et al., 2020), by relaxing the form of the prior, replacing the multivariate Dirac mass with a continuous distribution concentrated at zero (Ročková and George, 2018). Although these algorithms are fast to compute, they come at the sacrifice of interpretability, as posterior inclusion probabilities no longer guarantee the coefficient is zero but rather concentrated at zero. Beyond this, these algorithms only return a point estimate for β and therefore do not provide uncertainty quantification – a task at the heart of Bayesian inference.

To bridge the gap between scalability and uncertainty quantification several authors have turned to variational inference (VI). An approach to inference wherein the posterior distribution is approximated by a tractable family of distributions known as the variational family (see Zhang et al. (2019) for a review). In the context of high-dimensional Bayesian inference, VI has proven particularly successful, and has been employed in linear regression (Carbonetto and Stephens, 2012; Ormerod et al., 2017; Ray et al., 2020), logistic regression (Ray et al., 2020) and survival analysis (Komodromos et al., 2022) to name a few. Within the context of Bayesian group regression, to our knowledge only the Bayesian group LASSO has seen a variational counterpart (Babacan et al., 2014).

In this manuscript we examine the VB posterior arising from the group spike-and-slab prior with multivariate double exponential slab and Dirac spike, referring to our method as Group Spike-and-slab Variational Bayes (GSVB). We provide scalable variational approximations to three common classes of generalized linear models (GLMs): the Gaussian with identity link function, Binomial with logistic link function, and Poisson with exponential link function. We outline a general scheme for computing the variational posterior via co-ordinate ascent variational inference. Under which, we show for specific cases, that the variational family can be re-parameterized to allow for more efficient updates.

Through extensive numerical experiments it is shown that GSVB achieves state-of-the-art performance while significantly reducing computation time by several orders of magnitude compared to MCMC. Moreover, through our comparison to MCMC, we highlight that the variational posterior provides excellent uncertainty quantification through marginal credible sets with impressive coverage. Additionally, the proposed method is compared against the spike-and-slab group LASSO (Bai et al., 2020), a state-of-the-art Bayesian group selection algorithm that returns MAP estimates. Within this comparison our method demonstrates comparable or better performance in terms of group selection and effect estimation, whilst carrying the added benefit of providing uncertainty quantification, a feature not available by other scalable methods in the literature.

Finally, to highlight the practical utility of our method, we analyse three real datasets. In doing so, we demonstrate that our method provides excellent predictive accuracy, while also achieving parsimonious models. Additionally, we illustrate the usefulness of the VB posterior by showing its ability to provide posterior predictive intervals, a feature not available to methods that provide MAP estimates, and computationally prohibitive to compute via MCMC.

1.1 Notation

Let $y = (y_1, \dots, y_n)^\top \in \mathbb{R}^n$ denote the realization of the random vector $Y = (Y_1, \dots, Y_n)$. Further, let $X = (x_1, \dots, x_n)^\top \in \mathbb{R}^{n \times p}$ denote the design matrix, where for a group G_k let $X_{G_k} = (x_{1,G_k}, \dots, x_{n,G_k})^\top \in \mathbb{R}^{n \times m_k}$. Similarly, for $G_k^c = \{1, \dots, p\} \setminus G_k$, denote $X_{G_k^c} = (x_{1,G_k^c}, \dots, x_{n,G_k^c})^\top \in \mathbb{R}^{n \times (p-m_k)}$ where $x_{i,G_k^c} = \{x_{ij} : j \in G_k^c\}$, and $\beta_{G_k^c} = \{\beta_j : j \in G_k^c\}$. Wherein, without loss of generality we assume that the elements of the groups are ordered such that $1 = G_{1,1} < G_{1,2} < \dots < G_{M,m_M} = p$. Finally, denote D_{KL} as the Kullback-

Leibler divergence, defined as, $D_{\text{KL}}(Q\|P) = \int_{\mathcal{X}} \log\left(\frac{dQ}{dP}\right) dQ$, where Q and P are probability measures on \mathcal{X} , such that Q is absolutely continuous with respect to P .

2 Prior and Variational family

2.1 Group Spike-and-Slab prior

To model the coefficients β , we consider a group spike-and-slab prior. Under which for each group G_k , the prior over β_{G_k} consists of a mixture distribution of a multivariate Dirac mass on zero and a multivariate double exponential distribution, $\Psi(\beta_{G_k})$, whose density is given by,

$$\psi(\beta_{G_k}; \lambda) = C_k \lambda^{m_k} \exp(-\lambda \|\beta_{G_k}\|)$$

where $C_k = [2^{m_k} \pi^{(m_k-1)/2} \Gamma((m_k + 1)/2)]^{-1}$ and $\|\cdot\|$ is the ℓ_2 -norm. In the context of sparse Bayesian group regression the multivariate double exponential has been previously considered by [Raman et al. \(2009\)](#) and [Kyung et al. \(2010\)](#) as part of the Bayesian group LASSO. [Xu and Ghosh \(2015\)](#) first considered the use of this distribution as the slab within a group spike-and-slab prior.

Formally the prior, which we consider throughout, is given by $\Pi(\beta) = \bigotimes_{k=1}^M \Pi_k(\beta_{G_k})$, where each $\Pi_k(\beta_{G_k})$ has the hierarchical representation,

$$\begin{aligned} \beta_{G_k} | z_k &\stackrel{\text{ind}}{\sim} z_k \Psi(\beta_{G_k}; \lambda) + (1 - z_k) \delta_0(\beta_{G_k}) \\ z_k | \theta_k &\stackrel{\text{ind}}{\sim} \text{Bernoulli}(\theta_k) \\ \theta_k &\stackrel{\text{iid}}{\sim} \text{Beta}(a_0, b_0) \end{aligned} \tag{2}$$

for $k = 1, \dots, M$, where $\delta_0(\beta_{G_k})$ is the multivariate Dirac mass on zero with dimension $m_k = \dim(\beta_{G_k})$. In conjunction with the log-likelihood, $\ell(\mathcal{D}; \beta)$ for a dataset $\mathcal{D} = \{(y_i, x_i)\}_{i=1}^n$, we write the posterior density under the given prior as,

$$d\Pi(\beta|\mathcal{D}) = \Pi_D^{-1} e^{\ell(\mathcal{D}; \beta)} d\Pi(\beta) \tag{3}$$

where $\Pi_D = \int_{\mathbb{R}^p} e^{\ell(\mathcal{D}; \beta)} d\Pi(\beta)$ is a normalization constant known as the model evidence.

2.2 Variational Families

The posterior arising from the prior (2) and the dataset \mathcal{D} assigns probability mass to all 2^M possible sub-models, i.e. each subset $\mathcal{S} \subseteq \{1, \dots, M\}$, such that $z_k = 1, k \in \mathcal{S}$

and $z_k = 0$ otherwise. As using MCMC procedures to sample from this complex posterior distribution is computationally prohibitive, even for a moderate number of groups, we resort to variational inference to approximate it. This approximation is known as the variational posterior and is given by solving,

$$\tilde{\Pi} = \underset{Q \in \mathcal{Q}}{\operatorname{argmin}} D_{\text{KL}}(Q \| \Pi(\cdot | \mathcal{D})) \quad (4)$$

where \mathcal{Q} is the variational family.

For our purposes the variational family we consider is a mean-field variational family,

$$\mathcal{Q} = \left\{ Q(\mu, \sigma, \gamma) = \bigotimes_{k=1}^M Q_k(\mu_{G_k}, \sigma_{G_k}, \gamma_k) := \bigotimes_{k=1}^M [\gamma_k N_k(\mu_{G_k}, \operatorname{diag}(\sigma_{G_k}^2)) + (1 - \gamma_k)\delta_0] \right\} \quad (5)$$

where $\mu \in \mathbb{R}^p$ with $\mu_{G_k} = \{\mu_j : j \in G_k\}$, $\sigma^2 \in \mathbb{R}_+^p$ with $\sigma_{G_k}^2 = \{\sigma_j^2 : j \in G_k\}$, $\gamma = (\gamma_1, \dots, \gamma_M)^\top \in [0, 1]^M$. $N_k(\mu, \Sigma)$ denotes the multivariate Normal distribution with mean parameter μ and covariance Σ . Notably, under $Q \in \mathcal{Q}$, the vector of coefficients for each group G_k is a spike-and-slab distribution where the slab consists of the product of independent Normal distributions,

$$\beta_{G_k} \stackrel{\text{ind}}{\sim} \gamma_k \left[\bigotimes_{j \in G_k} N(\mu_j, \sigma_j^2) \right] + (1 - \gamma_k)\delta_0,$$

meaning the structure (correlations) between elements within the same group are not captured. To mitigate this, a second variational family is introduced, where the covariance within groups is unrestricted. Formally,

$$\mathcal{Q}' = \left\{ Q'(\mu, \Sigma, \gamma) = \bigotimes_{k=1}^M Q'_k(\mu_{G_k}, \Sigma_{G_k}, \gamma_k) := \bigotimes_{k=1}^M [\gamma_k N(\mu_{G_k}, \Sigma_{G_k}) + (1 - \gamma_k)\delta_0] \right\} \quad (6)$$

where $\Sigma \in \mathbb{R}^{p \times p}$ is a covariance matrix for which $\Sigma_{ij} = 0$, for $i \in G_k, j \in G_l, k \neq l$ and $\Sigma_{G_k} = (\Sigma_{ij})_{i,j \in G_k} \in \mathbb{R}^{m_k \times m_k}$ denotes the covariance matrix of the k th group. Notably, \mathcal{Q}' should provide greater flexibility when approximating the posterior, because unlike $\mathcal{Q} \subset \mathcal{Q}'$, it is able to capture the dependence between coefficients in the same group. The importance of which is highlighted empirically in Section 4 wherein the two families are compared.

Note that the posterior does not take the form Q or Q' , as the use of these variational families replaces the 2^M model weights by M VB group inclusion probabilities, γ_k , thereby introducing substantial additional independence. For example, information as to whether

two groups of variables are selected together or not is lost. However, the form of the VB approximation retains many of the interpretable features of the original posterior, for example, access to the posterior probabilities sub-models, and inclusion probabilities of particular groups.

3 Computing the Variational Posterior

Computing the variational posterior defined in (4) relies on optimizing a lower bound on the model evidence, $\Pi_{\mathcal{D}}$, known as the evidence lower bound (ELBO). The ELBO follows from the non-negativity of the Kullback-Leibler divergence and is given by $\mathbb{E}_Q [\ell(\mathcal{D}; \beta) - \log \frac{dQ}{d\Pi}]$. Intuitively, the first term evaluates the model’s fit to the data, while the second term acts as a regularizer, ensuring the variational posterior is “close” to the prior distribution.

Various strategies exist to tackle the minimization of the negative ELBO,

$$\mathcal{L}_Q(\mathcal{D}) := \mathbb{E}_Q \left[\log \frac{dQ}{d\Pi} - \ell(\mathcal{D}; \beta) \right] \quad (7)$$

with respect to $Q \in \mathcal{Q}$ (Zhang et al., 2019). One popular approach is co-ordinate ascent variational inference (CAVI), where sets of parameters of the variational family are optimized in turn while the remainder are kept fixed. Although this strategy does not (in general) guarantee the global optimum, it is easy to implement and often leads to scalable inference algorithms. In the following subsections we detail how this algorithm is constructed, noting that derivations are presented under the variational family \mathcal{Q}' , as the equations for $\mathcal{Q} \subset \mathcal{Q}'$ follow by restricting Σ_{G_k} to be a diagonal matrix.

3.1 Computing the Evidence lower bound

To compute the negative ELBO, note that the KL divergence between the prior and the variational distribution, $D_{\text{KL}}(Q' \parallel \Pi) = \mathbb{E}_{Q'} [\log(dQ'/d\Pi)]$ is constant regardless of the form of the likelihood. To evaluate an expression for this quantity the group independence structure between the prior and variational distribution is exploited, allowing for the log Radon-Nikodym, $\log(dQ'/d\Pi)$, to be expressed as,

$$\log \frac{dQ'}{d\Pi}(\beta) = \sum_{k=1}^M \log \frac{dQ'_k}{d\Pi_k}(\beta_{G_k}) = \sum_{k=1}^M \mathbb{I}_{z_k=1} \log \frac{\gamma_k dN_k}{\bar{w} d\Psi_k}(\beta_{G_k}) + \mathbb{I}_{z_k=0} \log \frac{(1 - \gamma_k) d\delta_0}{(1 - \bar{w}) d\delta_0}(\beta_{G_k}).$$

where $\bar{w} = \alpha_0/(\alpha_0 + b_0)$. Subsequently, it follows that,

$$D_{\text{KL}}(Q' \parallel \Pi) = \sum_{k=1}^M \left(\gamma_k \log \frac{\gamma_k}{\bar{w}} - \frac{\gamma_k}{2} \log(\det(2\pi \Sigma_{G_k})) - \frac{\gamma_k m_k}{2} - \gamma_k \log(C_k) \right. \\ \left. - \gamma_k m_k \log(\lambda) + \mathbb{E}_{Q'} [\mathbb{I}_{z_k=1} \lambda \|\beta_{G_k}\|] + (1 - \gamma_k) \log \frac{1 - \gamma_k}{1 - \bar{w}} \right) \quad (8)$$

where we have used the fact that $\mathbb{E}_{\beta_{G_k} \sim N(\mu_{G_k}, \Sigma_{G_k})}[(\beta_{G_k} - \mu_{G_k})^\top \Sigma_{G_k}^{-1} (\beta_{G_k} - \mu_{G_k})] = m_k$. Notably, there is no closed form for $\mathbb{E}_{Q'} [\mathbb{I}_{z_k=1} \lambda \|\beta_{G_k}\|]$, meaning $\mathcal{L}_{Q'}(\mathcal{D})$ is not tractable and optimization over this quantity would require costly Monte Carlo methods.

To circumvent this issue, a surrogate objective is constructed and used instead of the negative ELBO. This follows by applying Jensen's inequality to $\mathbb{E}_{Q'} [\mathbb{I}_{z_k=1} \lambda \|\beta_{G_k}\|]$, giving,

$$\mathbb{E}_{Q'} [\mathbb{I}_{z_k=1} \lambda \|\beta_{G_k}\|] = \gamma_k \mathbb{E}_{N_k} [\lambda \|\beta_{G_k}\|] \leq \gamma_k \lambda \left(\sum_{i \in G_k} \Sigma_{ii} + \mu_i^2 \right)^{1/2}. \quad (9)$$

Thus, $D_{\text{KL}}(Q' \parallel \Pi)$ can be upper-bounded by,

$$\varrho(\mu, \Sigma, \gamma) := \sum_{k=1}^M \left(\gamma_k \log \frac{\gamma_k}{\bar{w}} - \frac{\gamma_k}{2} \log(\det(2\pi \Sigma_{G_k})) - \frac{\gamma_k m_k}{2} \right. \\ \left. - \gamma_k \log(C_k) - \gamma_k m_k \log(\lambda) + \gamma_k \lambda \left(\sum_{i \in G_k} \Sigma_{ii} + \mu_i^2 \right)^{1/2} + (1 - \gamma_k) \log \frac{1 - \gamma_k}{1 - \bar{w}} \right) \quad (10)$$

and in turn, $\mathcal{L}_{Q'}(\mathcal{D}) \leq \varrho(\mu, \Sigma, \gamma) - \mathbb{E}_{Q'} [\ell(\mathcal{D}; \beta)]$. Via this upper bound, we are able to construct a tractable surrogate objective. Formally, this objective is denoted by, $\mathcal{F}(\mu, \Sigma, \gamma, \vartheta)$, where we introduce ϑ to parameterize additional hyperparameters, specifically those introduced to model the variance term under the Gaussian family, and those introduced to bound the Binomial likelihood. Under this parametrization we define,

$$\mathcal{F}(\mu, \Sigma, \gamma, \vartheta) := \varrho(\mu, \Sigma, \gamma) + \tilde{\varrho}(\vartheta) + \Lambda(\mu, \Sigma, \gamma, \vartheta) \geq \mathcal{L}_{Q'}(\mathcal{D}), \quad (11)$$

where $\tilde{\varrho}(\vartheta) : \Theta \rightarrow \mathbb{R}$ and $\Lambda(\mu, \Sigma, \gamma, \vartheta) \geq \mathbb{E}_{Q'} [-\ell(\mathcal{D}; \beta)]$ (which is an inequality under non-tractable likelihoods).

To this end, what remains to be computed is an expression for the expected negative log-likelihood and the term $\tilde{\varrho}(\vartheta)$ where appropriate. In the following three subsections we provide derivations of the objective function $\mathcal{F}(\mu, \Sigma, \gamma, \theta)$ for the Gaussian, Binomial and Poisson likelihoods taking the canonical link functions for each.

3.1.1 Gaussian

Under the Gaussian family with identity link function, $Y_i \stackrel{\text{iid}}{\sim} N(x_i^\top \beta, \tau^2)$ for all $i = 1, \dots, n$, the log-likelihood is given by $\ell(\mathcal{D}; \beta, \tau^2) = -\frac{n}{2} \log(2\pi\tau^2) - \frac{1}{2\tau^2} \|y - X\beta\|^2$. To model τ^2 an inverse Gamma prior is considered due to its popularity among practitioners, i.e. $\tau^2 \stackrel{\text{ind}}{\sim} \Gamma^{-1}(a, b)$ which has density $\frac{b^a}{\Gamma(a)} x^{-a-1} \exp(-\frac{b}{x})$ where $a, b > 0$. The prior is therefore given by $\Pi(\beta, \tau^2) = \Pi(\beta) \Gamma^{-1}(\tau^2)$, and the posterior density by $d\Pi(\beta, \tau^2 | \mathcal{D}) = \Pi_D^{-1} e^{\ell(\mathcal{D}; \beta, \tau^2)} d\Pi(\beta, \tau^2)$, where $\Pi_D = \int_{\mathbb{R}^p \times \mathbb{R}_+} e^{\ell(\mathcal{D}; \beta, \tau^2)} d\Pi(\beta, \tau^2)$ and $\mathcal{D} = \{(y_i, x_i)\}_{i=1}^n$ is the observed data.

To include this term within the inference procedure, the variational families \mathcal{Q} and \mathcal{Q}' are extended by $\mathcal{Q}_\tau = \mathcal{Q} \times \{\Gamma^{-1}(a', b') : a', b' > 0\}$ and $\mathcal{Q}'_\tau = \mathcal{Q}' \times \{\Gamma^{-1}(a', b') : a', b' > 0\}$ respectively. Under the extended variational family \mathcal{Q}'_τ , the negative ELBO is given by

$$\mathbb{E}_{Q'_\tau} \left[\log \frac{dQ'_\tau}{d\Pi}(\beta) + \log \frac{d\Gamma^{-1}(a', b')}{d\Gamma^{-1}(a, b)}(\tau^2) - \ell(\mathcal{D}; \beta, \tau^2) \right],$$

where the second term follows from the independence of τ^2 and β in the prior and variational family and is given by,

$$\tilde{\varrho}(\vartheta) := \mathbb{E}_{Q'_\tau} \left[\log \left(\frac{d\Gamma^{-1}(a', b')}{d\Gamma^{-1}(a, b)} \right) \right] = (a' - a)\kappa(a') + a \log \frac{b'}{b} + \log \frac{\Gamma(a)}{\Gamma(a')} + \frac{(b - b')a'}{b'} \quad (12)$$

where $\vartheta = \{(a', b')\}$. The expectation of the negative log-likelihood is given by,

$$\begin{aligned} \Lambda(\mu, \Sigma, \gamma, \vartheta) &:= \mathbb{E}_{Q'_\tau} [-\ell(\mathcal{D}; \beta)] = \frac{n}{2} (\log(2\pi) + \log(b') - \kappa(a')) \\ &+ \frac{a'}{2b'} \left(\|y\|^2 + \left(\sum_{i=1}^p \sum_{j=1}^p (X^\top X)_{ij} \mathbb{E}_{Q'_\tau} [\beta_i \beta_j] \right) - 2 \sum_{k=1}^M \gamma_k \langle y, X_{G_k} \mu_{G_k} \rangle \right) \end{aligned} \quad (13)$$

where,

$$\mathbb{E}_{Q'_\tau} [\beta_i \beta_j] = \begin{cases} \gamma_k (\Sigma_{ij} + \mu_i \mu_j) & i, j \in G_k \\ \gamma_k \gamma_h \mu_i \mu_j & i \in G_k, j \in G_h, h \neq k \end{cases} \quad (14)$$

Substituting (12) and (13) into (11) gives the objective $\mathcal{F}(\mu, \Sigma, \gamma, \theta)$ under the Gaussian family.

3.1.2 Binomial

Under the Binomial family with logistic link, $Y_i \stackrel{\text{iid}}{\sim} \text{Bernoulli}(p_i)$ for all $i = 1, \dots, n$ where $p_i = \mathbb{P}(Y_i = 1 | x_i) = \exp(x_i^\top \beta) / (1 + \exp(x_i^\top \beta))$. The log-likelihood is given by $\ell(\mathcal{D}, \beta) = \sum_{i=1}^n y_i (x_i^\top \beta) - \log(1 + \exp(x_i^\top \beta))$ where $\mathcal{D} = \{(y_i, x_i)\}_{i=1}^n$ with $y_i \in \{0, 1\}$.

Unlike the Gaussian family, variational inference in this setting is challenging because of the intractability of the expected log-likelihood under the variational family. To overcome this issue several authors have proposed bounds or approximations to maintain tractability (see [Depraetere and Vandebroek \(2017\)](#) for a review). Here we employ a bound introduced by [Jaakkola and Jordan \(1996\)](#), given as

$$s(x) \geq s(t) \exp \left\{ \frac{x-t}{2} - \frac{a(t)}{2}(x^2 - t^2) \right\} \quad (15)$$

where $s(x) = (1 + \exp(-x))^{-1}$ and $a(t) = \frac{s(t)-1/2}{t}$, $x \in \mathbb{R}$ and $t \in \mathbb{R}$ is an additional parameter that must be optimized to ensure tightness of the bound.

Using (15) allows for the negative log-likelihood to be bounded by,

$$-\ell(\mathcal{D}; \beta) \leq \sum_{i=1}^n -y_i x_i^\top \beta - \log s(t_i) + \frac{x_i^\top \beta + t_i}{2} + \frac{a(t_i)}{2}((x_i^\top \beta)^2 - t_i^2) \quad (16)$$

where $t_i \in \mathbb{R}$ is a hyper-parameter for each observation. Taking the expectation of (16) with respect to the variational family gives

$$\begin{aligned} \mathbb{E}_{Q'}[-\ell(\mathcal{D}; \beta)] \leq \Lambda(\mu, \Sigma, \gamma, \vartheta) := & \sum_{i=1}^n \left(\sum_{k=1}^M \gamma_k (1/2 - y_i) x_{i,G_k}^\top \mu_{G_k} \right) + \frac{t_i}{2} - \log s(t_i) \\ & + \frac{a(t_i)}{2} \left(\left(\sum_{j=1}^p \sum_{l=1}^p (x_{ij} x_{il} \mathbb{E}_{Q'}[\beta_j \beta_l]) \right) - t_i^2 \right) \end{aligned} \quad (17)$$

where $\vartheta = \{t_1, \dots, t_n\}$. In turn substituting (17) and $\tilde{\varrho}(\vartheta) = 0$ into (11) gives the objective under the Binomial family.

3.1.3 Poisson

Finally, under the Poisson family with exponential link function, $Y_i \stackrel{\text{iid}}{\sim} \text{Poisson}(\lambda_i)$ for all $i = 1, \dots, n$ with $\lambda_i = \exp(x_i^\top \beta) > 0$. The log-likelihood is given by, $\ell(\mathcal{D}; \beta) = \sum_{i=1}^n y_i x_i^\top \beta - \exp(x_i^\top \beta) - \log(y!)$, whose (negative) expectation is tractable and given by,

$$\mathbb{E}_{Q'}[-\ell(\mathcal{D}; \beta)] = \Lambda(\mu, \Sigma, \gamma, \vartheta) := \sum_{i=1}^n \log(y!) - M_{Q'}(x_i) + \left(\sum_{k=1}^M \gamma_k y_i x_{i,G_k}^\top \mu_{G_k} \right) \quad (18)$$

where $M_{Q'}(x_i) = \prod_{k=1}^M M_{Q_k}(x_{i,G_k})$ is the moment generating function under the variational family, with $M_{Q_k}(x_{i,G_k}) := \gamma_k M_{N_k}(x_{i,G_k}) + (1 - \gamma_k)$ being the moment generating function for the k th group and $M_{N_k}(x_{i,G_k}) = \exp \left\{ x_{i,G_k}^\top \mu_{G_k} + \frac{1}{2} x_{i,G_k}^\top \Sigma_{G_k} x_{i,G_k} \right\}$. Unlike the previous two families the Poisson family, does not require any additional variational parameters, therefore $\vartheta = \{\}$ and $\tilde{\varrho}(\vartheta) = 0$.

3.2 Coordinate ascent algorithm

Recall the aim is to approximate the posterior $\Pi(\cdot|\mathcal{D})$ by a distribution from a given variational family. This approximation is obtained via the minimization of the objective \mathcal{F} derived in the previous section. To achieve this a CAVI algorithm is proposed (Murphy, 2007; Blei et al., 2017). as outlined in Algorithm 1.

In this context, the objective introduced in (11) is written as $\mathcal{F}(\mu, \Sigma, \gamma, \vartheta) = \mathcal{F}(\mu_{G_k}, \mu_{G_k^c}, \Sigma_{G_k}, \Sigma_{G_k^c}, \gamma_k, \gamma_{-k}, \vartheta)$, highlighting the fact that optimization over the variational parameters occurs group-wise. Further, for each group k , while the optimization of the objective function over the inclusion probability, γ_k , can be done analytically, we use the Limited memory Broyden–Fletcher–Goldfarb–Shanno optimization algorithm (L-BFGS) to update μ_{G_k} at each iteration of the CAVI procedure. Details for the optimization with respect to Σ_{G_k} are presented in Section 3.2.1. The hyper-parameters, ϑ , are updated using L-BFGS for the Gaussian family and analytically for those under the Binomial family.

Algorithm 1 Group sparse co-ordinate ascent variational inference

Initialize $\mu, \Sigma, \gamma, \vartheta$

while not converged

for $k = 1, \dots, M$

$\mu_{G_k} \leftarrow \operatorname{argmin}_{\mu_{G_k} \in \mathbb{R}^{m_k}} \mathcal{F}(\mu_{G_k}, \mu_{G_k^c}, \Sigma_{G_k}, \Sigma_{G_k^c}, \gamma_k = 1, \gamma_{-k}, \vartheta)$

$\Sigma_{G_k} \leftarrow \operatorname{argmin}_{\Sigma_{G_k} \in \mathbb{R}^{m_k \times m_k}} \mathcal{F}(\mu_{G_k}, \mu_{G_k^c}, \Sigma_{G_k}, \Sigma_{G_k^c}, \gamma_k = 1, \gamma_{-k}, \vartheta)$

$\gamma_k \leftarrow \operatorname{argmin}_{\gamma_k \in [0,1]} \mathcal{F}(\mu_{G_k}, \mu_{G_k^c}, \Sigma_{G_k}, \Sigma_{G_k^c}, \gamma_k, \gamma_{-k}, \vartheta)$

$\vartheta \leftarrow \operatorname{argmin}_{\vartheta \in \Theta} \mathcal{F}(\mu_{G_k}, \mu_{G_k^c}, \Sigma_{G_k}, \Sigma_{G_k^c}, \gamma_k, \gamma_{-k}, \vartheta)$

return $\mu, \Sigma, \gamma, \vartheta$.

To assess convergence, the total absolute change in the parameters is tracked, terminating when this quantity falls below a specified threshold, set to 10^{-3} in our implementation. Other methods involve monitoring the absolute change in the ELBO, however we found this prohibitively expensive to compute for this purpose.

3.2.1 Re-parameterization of Σ_{G_k}

Our focus now turns to the optimization of $\mathcal{F}(\mu_{G_k}, \mu_{G_k^c}, \Sigma_{G_k}, \Sigma_{G_k^c}, \gamma_k = 1, \gamma_{-k}, \vartheta)$ w.r.t. Σ_{G_k} . By using similar ideas to those of Seeger (1999) and Oppé and Archambeau (2009), it can

be shown that only one free parameter is needed to describe the optimum of Σ_{G_k} under the Gaussian and Binomial family. Below, we outline this process for both the Gaussian and Poisson families, and present the details for the Binomial family in Section A of the Supplementary material.

The objective w.r.t Σ_{G_k} under the Gaussian family, is given by,

$$\frac{a'}{2b'} \text{tr}(X_{G_k}^\top X_{G_k} \Sigma_{G_k}) - \frac{1}{2} \log \det \Sigma_{G_k} + \lambda \left(\sum_{i \in G_k} \Sigma_{ii} + \mu_i^2 \right)^{1/2} + C \quad (19)$$

where C is a constant that does not depend on Σ_{G_k} . Differentiating (19) w.r.t. Σ_{G_k} , setting to zero and re-arranging gives,

$$\Sigma_{G_k} = \left(\frac{a'}{b'} X_{G_k}^\top X_{G_k} + 2\nu_k I_{m_k} \right)^{-1} \quad (20)$$

where $\nu_k = \frac{1}{2} \lambda (\sum_{i \in G_k} \Sigma_{ii} + \mu_i^2)^{-1/2}$. Thus, substituting $\Sigma_{G_k} = \left(\frac{a'}{b'} X_{G_k}^\top X_{G_k} + w_k I_{m_k} \right)^{-1}$ where $w_k \in \mathbb{R}$ into the objective and optimizing over w_k is equivalent to optimizing over Σ_{G_k} , and carries the added benefit of requiring one free parameter to perform rather than $m_k(m_k - 1)/2$. Note that under this re-parametrization the inversion of an $m_k \times m_k$ matrix is required which can be a time consuming operation for large m_k .

For the Poisson family the same re-parameterization cannot be used, so Σ_{G_k} is parameterized by $U_k^\top U_k$ where $U_k \in \mathbb{R}^{m_k \times m_k}$ is an upper triangular matrix. Optimization is then performed on the upper triangular elements of U_k , for which we use L-BFGS in our implementation.

3.2.2 Initialization

As with any gradient-descent based approach, our CAVI algorithm is sensitive to the choice of initial values. We suggest to initialize μ using the group LASSO from the package `gglasso` using a small regularization parameter. This ensures many of the elements are non-zero. The covariance matrix Σ can be initialised by using the re-parametrization outlined in Section 3.2.1 with an initial value of $w_k = 1$ for $k = 1, \dots, M$ for both the Gaussian and the Binomial families. For the Poisson family we propose the use of an initial covariance matrix $\Sigma = \text{diag}(0.2, \dots, 0.2)$. Finally, the inclusion probabilities are initialised as $\gamma = (0.5, \dots, 0.5)^\top$. The following initial values for the additional hyper-parameters ϑ are used: $a' = b' = 10^{-3}$ and $t_i = \left(\sum_{k=1}^M \gamma_k [\langle \mu_{G_k}, x_{i,G_k} \rangle^2 + x_{i,G_k}^\top \Sigma_{G_k} x_{i,G_k}] \right)^{1/2}$ for all $i = 1, \dots, n$.

4 Numerical experiments

In this section a numerical evaluation of our method, referred to as Group Spike-and-slab Variational Bayes (GSVB), is presented. Where necessary we distinguish between the two families, \mathcal{Q} and \mathcal{Q}' , by the suffix ‘-D’ and ‘-B’ respectively, i.e. GSVB-D denotes the method under the variational family \mathcal{Q} . Notably, throughout all our numerical experiments the prior parameters are set to $\lambda = 1$, $\alpha_0 = 1$, $b_0 = M$, and $a = b = 10^{-3}$ for the inverse-Gamma prior on τ^2 under the Gaussian family.

This section begins with a comparison of GSVB against MCMC to assess the quality of the variational posterior in terms of variable selection and uncertainty quantification. Following this, a large-scale comparison with the Spike-and-Slab Group LASSO (SSGL), a state-of-the-art MAP Bayesian group selection method described in detail in Section 4.3, is performed.

4.1 Simulation set-up

Data is simulated for $i = 1, \dots, n$ observations each having a response $y_i \in \mathbb{R}$ and p continuous predictors $x_i \in \mathbb{R}^p$. The response is sampled independently from the respective family with mean given by $f(\beta_0^\top x_i)$ where f is the link function (and variance applicable to the Gaussian family of $\tau^2 = 1$). The true coefficient vector $\beta_0 = (\beta_{0,G_1}, \dots, \beta_{0,G_M})^\top \in \mathbb{R}^p$ consists of M groups each of size m i.e. $M \times m = p$. Of these groups, s are chosen at random to be non-zero and have each of their element values sampled independently and uniformly from $[-\beta_{\max}, 0.2] \cup [0.2, \beta_{\max}]$ where $\beta_{\max} = 1.5, 1.0$ and 0.45 for the Gaussian, Binomial and Poisson families respectively. Finally, the predictors are generated from one of four settings:

- **Setting 1:** $x_i \stackrel{\text{iid}}{\sim} N(0_p, I_p)$ where 0_p is the p -dimension zero vector and I_p the $p \times p$ identity matrix.
- **Setting 2:** $x_i \stackrel{\text{iid}}{\sim} N(0_p, \Sigma)$ where $\Sigma_{ij} = 0.6^{|i-j|}$ for $i, j = 1, \dots, p$.
- **Setting 3:** $x_i \stackrel{\text{iid}}{\sim} N(0, \Sigma)$ where Σ is a block diagonal matrix where each block A is a 50×50 square matrix such that $A_{jl} = 0.6, j \neq l$ and $A_{jj} = 1$ otherwise.
- **Setting 4:** $x_i \stackrel{\text{iid}}{\sim} N(0, \Sigma)$ where $\Sigma = (1 - \alpha)W^{-1} + \alpha V^{-1}$ with $W \sim \text{Wishart}(p + \nu, I_p)$ and V is a block diagonal matrix of M blocks, where each block V_k , for $k = 1, \dots, M$,

is an $m_k \times m_k$ matrix given by $V_k \sim \text{Wishart}(m_k + \nu, I_{m_k})$; we let $(\nu, \alpha) = (3, 0.9)$ so that predictors within groups are more correlated than variables between different groups.

To evaluate the performance of the methods four different metrics are considered:

- (i) the ℓ_2 -error, $\|\hat{\beta} - \beta_0\|_2$, between the true vector of coefficients and the estimated coefficient $\hat{\beta}$ defined as the posterior mean where applicable, or the maximum a posteriori (MAP) estimate if this is returned,
- (ii) the area under the curve (AUC) of the receiver operator characteristic curve, which compares true positive and false positive rate for different thresholds of the group posterior inclusion probability,
- (iii) the marginal coverage of the non-zero coefficients, which reports the proportion of times the true coefficient $\beta_{0,j}$ is contained in the marginal credible set for $j \in \{j : \beta_{0,j} \neq 0\}$,
- (iv) and the size of the marginal credible set for the non-zero coefficients, given by the Lebesgue measure of the set.

The last two metrics can only be computed when a distribution for β is available i.e. via MCMC or VB. The 95% ($\alpha = 0.95$) marginal credible sets for each variable $j \in G_k$ for $k = 1, \dots, M$ are computed by GSVB by:

$$S_j = \begin{cases} \{0\} & \text{if } \gamma_k < \alpha \\ \left[\mu_j \pm \Sigma_{jj}^{1/2} \Phi^{-1}\left(\frac{\alpha_{\gamma_k}}{2}\right) \right] & \text{if } \gamma_k \geq \alpha \text{ and } 0 \notin [\mu_j \pm \Sigma_{jj}^{1/2} \Phi^{-1}\left(\frac{\alpha_{\gamma_k}}{2}\right)] \\ \left[\mu_j \pm \Sigma_{jj}^{1/2} \Phi^{-1}\left(\frac{\alpha_{\gamma_k}}{2} + \frac{1-\gamma_k}{2}\right) \right] \cup \{0\} & \text{otherwise} \end{cases}$$

where $\alpha_{\gamma_k} = 1 - \frac{\alpha}{\gamma_k}$ and Φ^{-1} is the quantile function of the standard Normal distribution.

4.2 Comparison to MCMC

Our first numerical study compares GSVB to the posterior obtained via MCMC, often considered the gold standard in Bayesian inference. The details of the MCMC sampler used for this comparison are outlined in Section C of the Supplementary material¹. The MCMC sampler is ran for 100,000 iterations taking a burn-in period of 50,000 iterations.

¹An implementation is available at <https://github.com/mkomod/sps1>.

Within this comparison we set $p = 1,000$, $m = 5$, and vary the number of non-zero groups, s . As highlighted in Figure 1 GSVB-B performs excellently in nearly all settings, demonstrating comparable results to MCMC in terms of ℓ_2 -error and AUC. This indicates that GSVB-B exhibits similar characteristics to MCMC, both in terms of the selected groups and the posterior mean. As anticipated, all the methods exhibit better performance in simpler settings and show a slight decline in performance as the complexity of the problem increases.

Regarding coverage, whilst MCMC shows slightly better performance compared to GSVB, the proposed method still provides credible sets that capture a significant portion of the true non-zero coefficients (particularly GSVB-B). However, the credible sets of the variational posterior are sometimes not large enough to capture the true non-zero coefficients. This observation is further supported by the size of the marginal credible sets, with MCMC producing the largest sets, followed by GSVB-B and GSVB-D. These findings confirm the well-known fact that VB tends to underestimate the posterior variance (Carbonetto and Stephens, 2012; Blei et al., 2017; Zhang et al., 2019; Ray et al., 2020).

Interestingly, it is noticed that the set size is increased under \mathcal{Q}' , highlighting the fact that the mean field variational family is lacking the necessary flexibility to accurately capture the underlying structure in the data. Furthermore, this result indicates that the full marginal credible quantity improves through the consideration of the interactions within the group.

4.3 Large scale simulations

In this section, our proposed approach is compared against the spike-and-slab group LASSO (SSGL) proposed by Bai et al. (2020) a state-of-the-art Bayesian method. Notably, SSGL employs a similar prior to that introduced in (2), however the multivariate Dirac mass on zero is replaced with a multivariate double exponential distribution, giving a continuous mixture with one density acting as the spike and the other as the slab, parameterized by λ_0 and λ_1 respectively. Under this prior Bai et al. (2020) derive an EM algorithm, which allows for fast updates, however, only MAP estimates are returned, meaning a posterior distribution for β is not available. In addition, the performance of the proposed method is evaluated on larger datasets. As both methods are scalable with p , in the comparisons of this section p is increased to $p = 5,000$. Both the sample size and the number of active

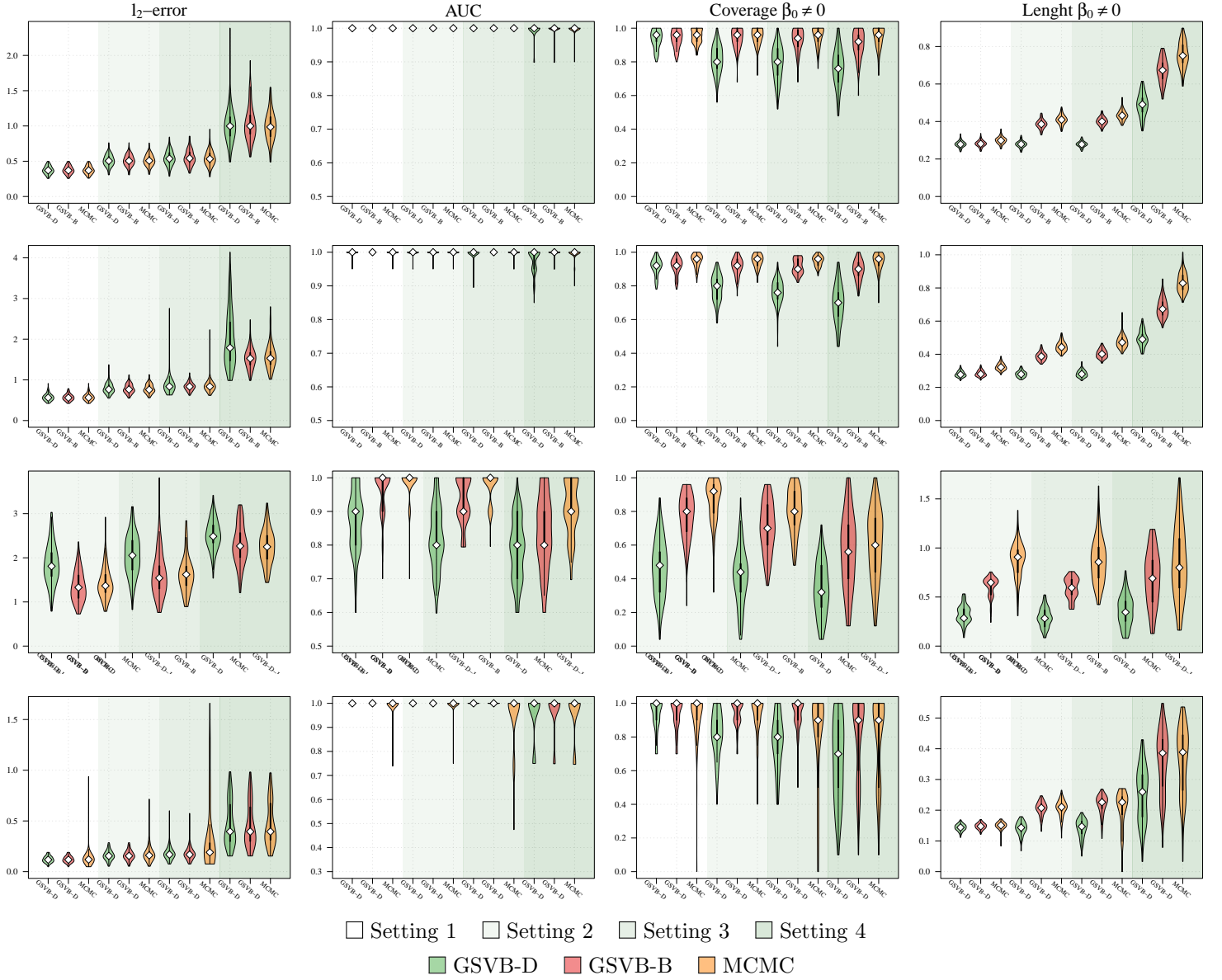


Figure 1: Performance evaluation of GSVB and MCMC for Settings 1–4 with $p = 1,000$ across 100 runs. For each method the white diamond (\diamond) indicates the median of the metric, the thick black line (—) the interquartile range, and the black line (—) 1.5 times the interquartile range. **Rows 1–2:** Gaussian family with $(n, m, s) = (200, 5, 5), (200, 5, 10)$. **Row 3:** Binomial family with $(n, m, s) = (400, 5, 5)$. **Row 4:** Poisson family with $(n, m, s) = (400, 5, 2)$. Note that for the Binomial family Setting 1 results in perfect separation of classes and is excluded from the study

(non-zero) groups, s are varied as illustrated in Figure 2.

In this comparison, we set $\lambda_1 = 1$ for SSGL meaning the slab is identical between the two methods. For the spike for SSGL we took a value of $\lambda_0 = 100$ for the Gaussian and Poisson family and $\lambda_0 = 20$ under the Binomial family. These values were selected to ensure that sufficient mass is concentrated about zero without turning to cross validation to select the value. Finally, we let $a_0 = 1$ and $b_0 = M$ for both methods as in the previous section.

Given that SSGL only returns a point estimate for the vector of coefficients β , the methods are compared in terms of ℓ_2 -error between the estimated coefficient and the true one, as well as in terms of AUC using the group inclusion probabilities. Overall GSVB performs comparatively or better than SSGL in most settings, obtaining a lower ℓ_2 -error and higher AUC (Figure 2). As expected, across the different methods there is a decrease in performance as the difficulty of the setting increases, meaning all methods perform better when there is less correlation in the design matrix. We note that the runtime of SSGL is marginally faster than our method in Settings 1-3, and faster in Settings 4. This is explained by the fact that SSGL only provides point estimate for β , rather than the full posterior distribution. A full breakdown of the runtimes is presented in Section D.2 of the Supplementary Materials.

Within this large scale simulation our method provides excellent uncertainty quantification across the different settings. In particular, GSVB-B provides better coverage of the non-zero coefficients than GSVB-D, which can be justified by the set size. As in our comparison to MCMC we notice that there is an increase in the posterior set size as the difficulty of the setting increases, i.e. when there is an increase in the correlation of the design matrix.

5 Real data analysis

Here we conduct an analysis of three real world datasets. The first two of which are linear regression problems wherein $p \gg n$ for which GSVB and SSGL are applied. The third is a logistic regression problem where $p < n$, for which the logistic group LASSO is applied in addition to GSVB and SSGL. As before, GSVB was ran with a value of $\lambda = 1$, $a_0 = 1$ and $b_0 = M$. For SSGL, a value of $\lambda_1 = 1$ was used and λ_0 was chosen via five fold cross

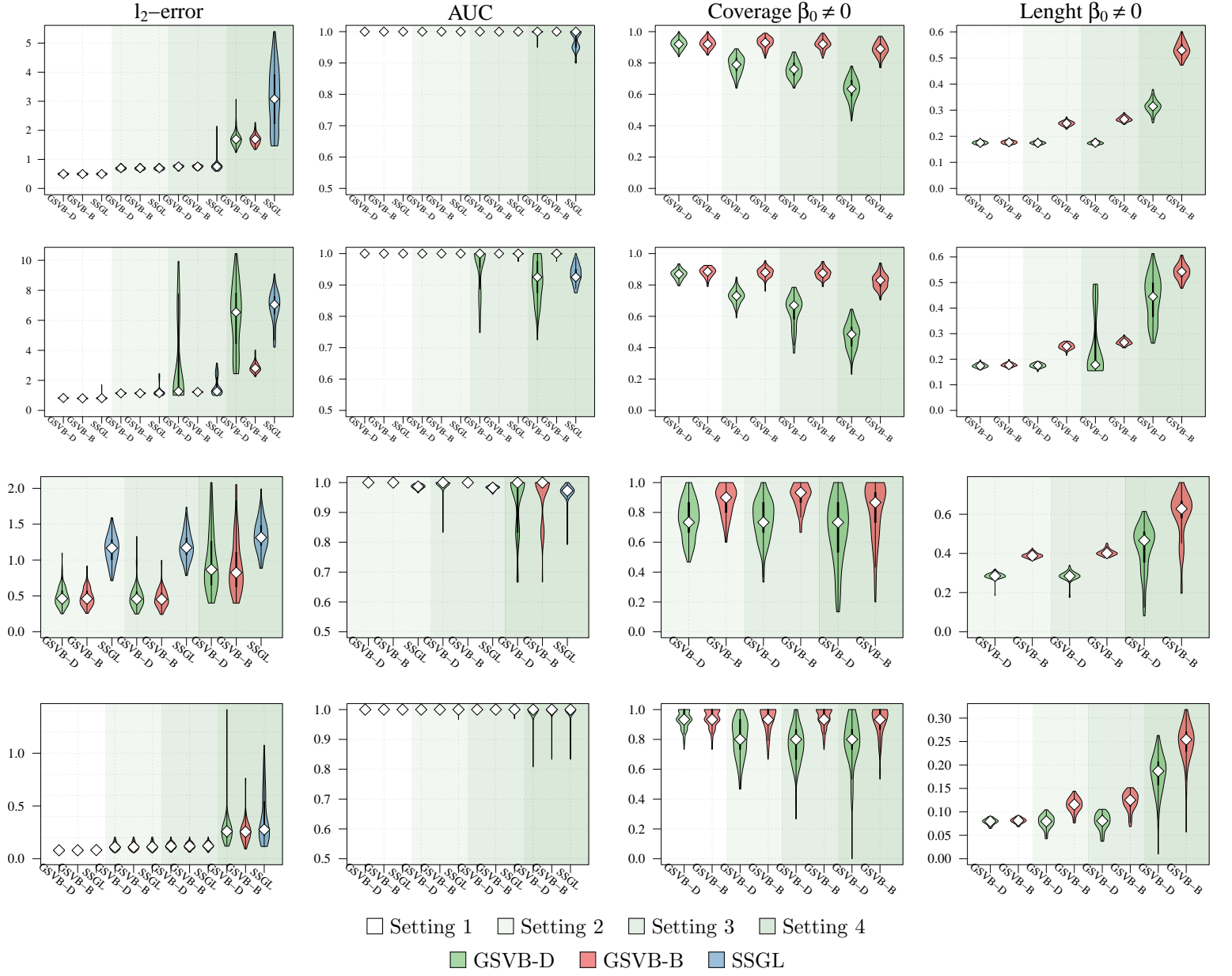


Figure 2: Performance evaluation of GSVB and SSGL for Settings 1–4 with $p = 5,000$ across 100 runs. For each method the white diamond (\diamond) indicates the median of the metric, the thick black line (—) the interquartile range, and the black line (—) 1.5 times the interquartile range. **Rows 1 – 2:** Gaussian family with $(n, m, s) = (500, 10, 10), (500, 10, 20)$. **Row 3:** Binomial family with $(n, m, s) = (1000, 5, 5)$. **Row 4:** Poisson family with $(n, m, s) = (1000, 5, 3)$. Note that for the Binomial family Setting 1 results in perfect separation of classes and is excluded from the study.

validation performed with the training set, the same values for a_0 and b_0 were used.

Overall, our results highlight that GSVB achieves state-of-the-art performance, producing parsimonious models with excellent predictive accuracy. Furthermore, in our analysis of the first two datasets, variational posterior predictive distributions are constructed. These highlight the practical utility of the method, demonstrating how uncertainty in the predictions is quantified – an added benefit that is otherwise not available via MAP methods such as SSGL.

5.1 Genetic determinants of Low-density Lipoprotein in mice

The first dataset analyzed is from the Mouse Genome Database (Blake et al., 2021) and consists of $p = 10,346$ single nucleotide polymorphisms (SNPs) collected from $n = 1,637$ laboratory mice. Notably, each SNP, x_{ij} for $j = 1, \dots, p$ and $i = 1, \dots, n$, takes a value of 0, 1 or 2. This value indicates how many copies of the risk allele are present. Alongside the genotype data, a phenotype (response) is also collected. The phenotype we consider is low-density lipoprotein cholesterol (LDL-C), which has been shown to be a major risk factor for conditions like coronary artery disease, heart attacks, and strokes (Silverman et al., 2016).

To pre-process the original dataset SNPs with a rare allele frequency, given by $\text{RAF}_j = \frac{1}{2n} \sum_{i=1}^n (\mathbb{I}(x_{ij} = 1) + 2\mathbb{I}(x_{ij} = 2))$ for $j = 1, \dots, p$, below the first quartile were discarded. Further, due to the high collinearity, covariates with $|\text{corr}(x_j, x_k)| \geq 0.97$ for $k > j$, $j = 1, \dots, p - 1$, were removed. After pre-processing, 3,341 SNPs remained. These were used to construct groups by coding each $x_{ij} : \{0, 1, 2\} \mapsto \{(0, 0), (0, 1), (1, 1)\}$, in turn giving groups of size $m = 2$.

To evaluate the methods ten fold cross validation is used. Specifically, methods are fit to the validation set and the test set is used for evaluation. This is done by computing the: (i) MSE between the true and predicted value of the response, given by $\frac{1}{\tilde{n}} \|y - X\hat{\beta}\|^2$ where \tilde{n} is the size of the test set, (ii) posterior predictive (PP) coverage, which measures the proportion of times the response is included in the 95% PP set, and (iii) the average size of the 95% PP set. In addition, (iv) the number of groups selected, given by $\sum_{k=1}^M \mathbb{I}(\gamma_k > 0.5)$ is also reported.

Importantly the PP distribution is available for GSVB, and given by, $\tilde{p}(y^*|x^*, \mathcal{D}) = \int_{\mathbb{R}^p \times \mathbb{R}^+} p(y^*|\beta, \tau^2, x^*, \mathcal{D}) d\tilde{\Pi}(\beta, \tau^2)$ where $x^* \in \mathbb{R}^p$ is a feature vector (see Section B of

the Supplementary material for details). In genetics studies, $x^{*\top}\beta$, is referred to as the polygenic risk score and is commonly used to evaluate genetic risk. While frequentist or MAP methods offer only point estimates, Figure 3 demonstrates that GSVB can offer a distribution for this score, highlighting the uncertainty associated with the estimate.

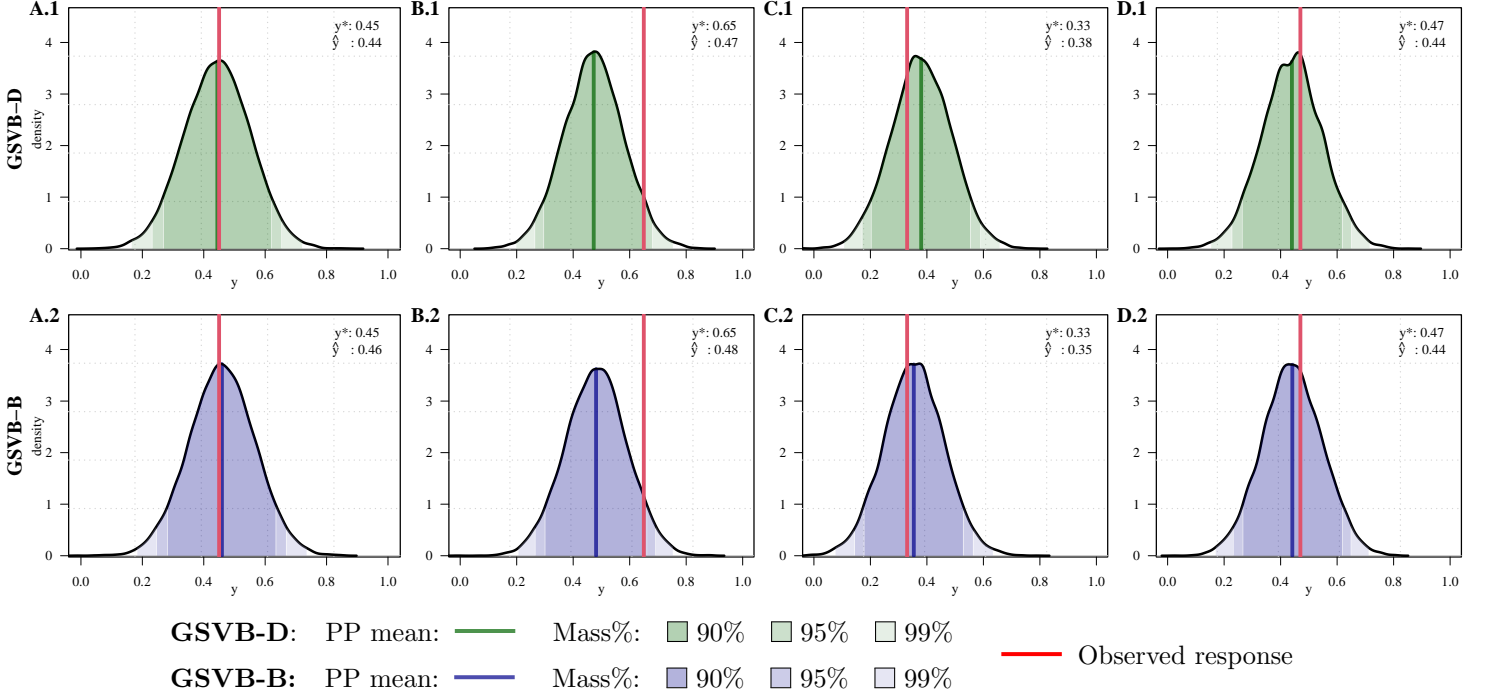


Figure 3: *Genetic determinants of LDL-C in mice*, variational posterior predictive distribution for GSVB-D (panels A.1 - D.1) and GSVB-B (panels A.2 - D.2) constructed for four observations in the held out test set (fold 1). Notably the red line (—) represents the measured LDL-C level, with the adjacent text giving this value (y^*) and the posterior mean (\hat{y}). The shading of the variational posterior indicates where 90%, 95% and 99% of the mass is contained.

Regarding the performance of each method results are presented in Table 1, these highlight that GSVB performs excellently obtaining parsimonious models with a comparable MSE to SSGL. In addition, GSVB provides impressive uncertainty quantification, yielding a coverage of 0.945 and 0.941 for GSVB-D and GSVB-B respectively. The SNPs selected by GSVB-D and GSVB-B are similar and reported in Table 6 of the Supplementary material. When the methods are fit to the full dataset, the SNPs selected by both method are: **rs13476241**, **rs13477968**, and **rs13483814**, with GSVB-B selecting **rs13477939** in

addition. Notably, **rs13477968** corresponds to the *Ago3* gene, which has been shown to play a role in activating LDL receptors, which in turn regulate LDL-C (Matsui et al., 2010).

Method	MSE	Num. selected groups	PP. coverage	PP. length
GSVB-D	0.012 (0.002)	3.50 (0.527)	0.945 (0.027)	0.425 (0.005)
GSVB-B	0.012 (0.002)	4.00 (0.667)	0.941 (0.029)	0.421 (0.005)
SSGL	0.012 (0.002)	57.40 (5.481)	-	-

Table 1: *Genetic determinants of LDL-C in mice*, evaluation of methods on the held out genotype data. Reported is the 10 fold cross validated MSE, the number of selected groups, the posterior predictive coverage, and mean posterior predictive interval length.

5.2 Bardet-Biedl Syndrome Gene Expression Study

The second dataset we examine is of microarray data, consisting of gene expression measurements for 120 laboratory rats². Originally the dataset was studied by Scheetz et al. (2006) and has subsequently been used to demonstrate the performance of several group selection algorithms (Huang and Zhang, 2010; Breheny and Huang, 2015; Bai et al., 2020). Briefly, the dataset consists of normalized microarray data harvested from the eye tissue of 12 week old male rats. The outcome of interest is the expression of TRIM32 a gene known to cause Bardet-Biedl syndrome, a genetic disease of multiple organs including the retina.

To pre-process the original dataset, which consists of 31,099 probe sets (the predictors), we follow Breheny and Huang (2015) and select the 5,000 probe sets which exhibit the largest variation in expression on the log scale. Further, following Breheny and Huang (2015) and Bai et al. (2020) a non-parametric additive model is used, wherein, $y_i = \mu + \sum_{j=1}^p f_j(x_{ij}) + \epsilon_i$ with $\epsilon_i \sim N(0, \tau^2)$ and $f_j : \mathbb{R} \rightarrow \mathbb{R}$. Here, $y_i \in \mathbb{R}$ corresponds to the expression of TRIM32 for the i th observation, and x_{ij} the expression of the j th probe set for the i th observation. To approximate f_j a three term natural cubic spline basis expansion is used. The resulting processing gave a group regression problem with $n = 120$ and $M = 1,000$ groups of size $m = 3$, written as,

$$y_i = \mu + \sum_{j=1}^M \sum_{k=1}^m \phi_{j,k}(x_{ij}) + \epsilon_i \quad (21)$$

²available at <ftp://ftp.ncbi.nlm.nih.gov/geo/series/GSE5nnn/GSE5680/matrix/>

where $\phi_{j,k}$ is the k th basis for f_j .

The performance of the methods are evaluated as in Section 5.1, similarly averaged over 10 folds. Overall, GSVB performed excellently, in particular GSVB-D obtained a smaller 10-fold cross validated MSE and model size than SSGL, meaning the models produced are parsimonious and comparably predictive to those of SSGL (Table 2). Furthermore, the PP coverage is excellent, particularly for GSVB-D which has a larger PP coverage than GSVB-B, whilst also having a smaller PP interval length.

Method	MSE	Num. selected groups	PP. coverage	PP. length
GSVB-D	0.017 (0.019)	1.10 (0.316)	0.983 (0.035)	0.5460 (0.100)
GSVB-B	0.018 (0.013)	1.50 (0.527)	0.950 (0.070)	0.5673 (0.091)
SSGL	0.019 (0.001)	2.30 (1.060)	—	—

Table 2: *Bardet-Biedl Syndrome Gene Expression Study*, evaluation of methods. Presented is the average (sd.) over the 10 folds for the: mean squared error, number of selected groups, posterior predictive coverage, and mean posterior predictive interval length. These values are computed for the held out test set. Notably, GSVB failed to converge on the third fold.

To identify genes associated with *TRIM32* expression, GSVB was ran on the full dataset. Notably, both methods identify one gene each, with GSVB-D identifying *Clec3a* and GSVB-B identifying *Slc25a34*. Interestingly, the MSE was 0.012 and 0.008 for each method, suggesting *Slc25a34* is more predictive of *TRIM32* expression. Further, the PP coverage was 0.960 for both methods and the PP interval length was 0.460 and 0.367 for GSVB-D and GSVB-B, reflecting there is less uncertainty in the prediction under GSVB-B.

5.3 MEMset splice site detection

The following application is based around the prediction of short read DNA motifs, a task which plays an important role in many areas of computational biology. For example, in gene finding, wherein algorithms such as GENIE (Burge and Karlin, 1997) rely on the prediction of splice sites (regions between coding (exons) and non-coding (introns) DNA

segments).

The MEMset donor data has been used to build predictive models for splice sites and consists of a large training and test set³. The original training set contains 8,415 true and 179,438 false donor sites and the test set 4,208 true and 89,717 false donor sites. The predictors are given by 7 factors with 4 levels each (A, T, C, G), a more detailed description of which is given in [Yeo and Burge \(2004\)](#). Initially analyzed by [Yeo and Burge \(2004\)](#), the data has subsequently been used by [Meier et al. \(2008\)](#) to evaluate the logistic group LASSO.

To create a predictive model we follow [Meier et al. \(2008\)](#) and consider all 3rd order interactions of the 7 factors, which gives a total of $M = 64$ groups and $p = 1,156$ predictors. To balance the sets we randomly sub-sampled the training set without replacement, creating a training set of 1,500 true ($Y = 1$) and 1,500 false donor sites. Regarding the test set a balanced set of 4,208 true and 4,208 false donor sites was created.

In addition to GSVB, we fit the SSGL and the group LASSO (used in the original analysis), for which we performed 5-fold cross validation to tune the hyperparameters. To assess the different methods, we use the test data, dividing it into 10 folds, and reporting the: (i) precision ($\frac{TP}{TP + FP}$), (ii) recall ($\frac{TP}{TP + FN}$), (iii) F-score ($\frac{TP}{TP + 0.5FP + 0.5FN}$), (iv) AUC, and (v) the maximum correlation coefficient between true class membership and the predicted membership over a range of thresholds, ρ_{\max} , as used in [Yeo and Burge \(2004\)](#) and [Meier et al. \(2008\)](#). In addition we report (vi) the number selected groups, which for the group LASSO is given by the number which have a non-zero $\ell_{2,1}$ norm.

Overall the methods performed comparably. With GSVB-D obtaining the largest recall and the group LASSO the largest precision, F-score, AUC, and ρ_{\max} by a small margin (Table 3). However, GSVB returned models that were of smaller size and therefore more parsimonious than those of SSGL and the group LASSO. This is further highlighted in Figure 4, which showcases the fact that the models obtained by GSVB are far simpler, selecting groups 1–7 as well as the interactions between groups 2:4 and 6:7 for both methods, with GSVB-D selecting 5:7 and GSVB-B selecting 2:6, 4:6 and 2:4:6 in addition to these. Further, Figure 4 showcases the fact that uncertainty is available about the norms of the groups.

³available at <http://hollywood.mit.edu/burgelab/maxent/ssdata/>

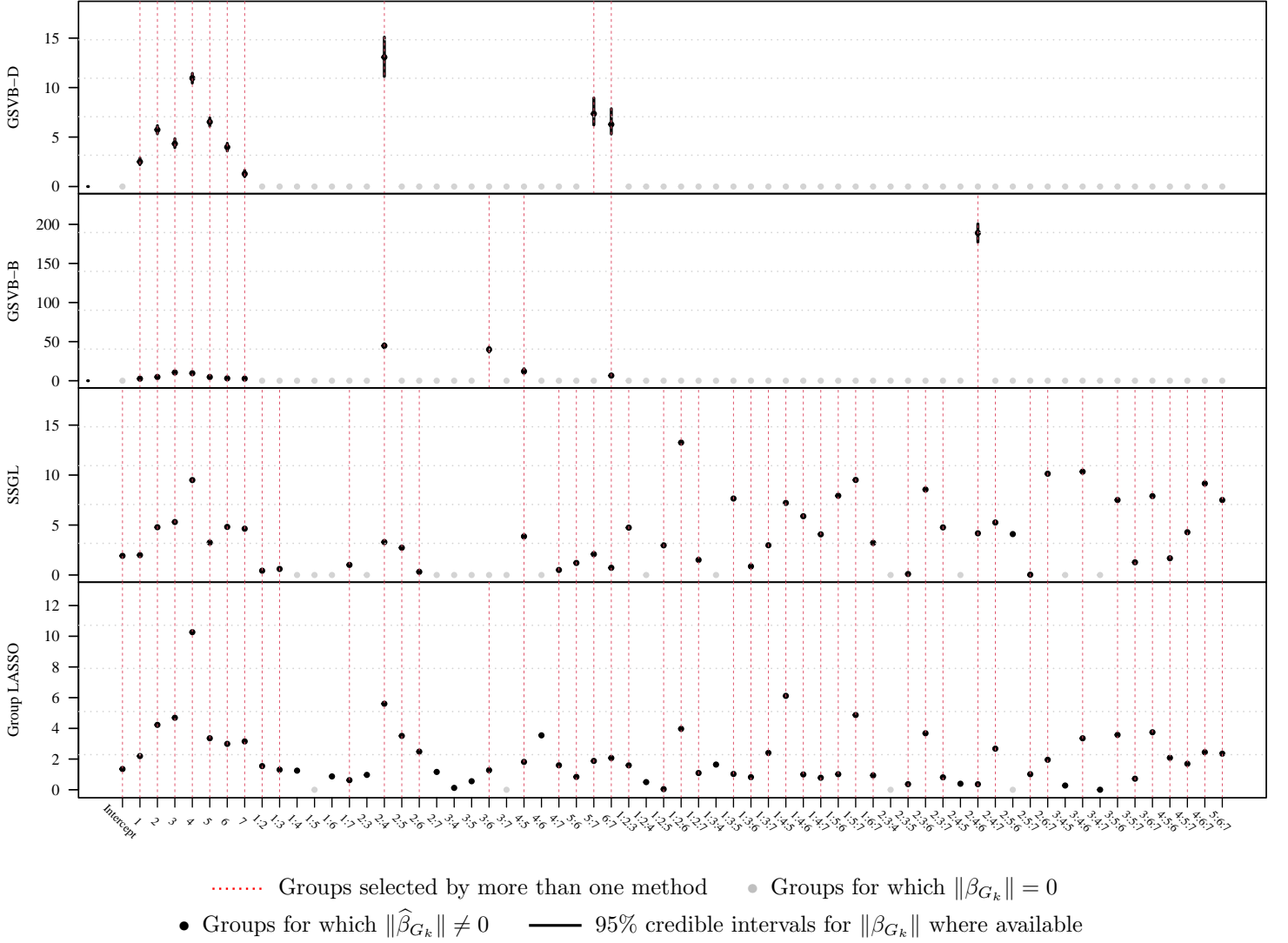


Figure 4: *MEMset splice site detection*, comparison of ℓ_2 -norms for each group of coefficients $\hat{\beta}_{G_k}$ for $k = 1, \dots, 64$. The red dotted line (.....) shows groups which have been selected by more than one method. The points indicate $\|\hat{\beta}_{G_k}\|$ where $\hat{\beta}_{G_k}$ is the posterior mean for GSVB, the MAP for SSGL and the MLE estimate under the group LASSO. The points are coloured in black (•) when they are non-zero and grey (•) otherwise. Finally when available the 95% credible set for $\|\beta_{G_k}\|$ is given by the solid black line (—).

Method	Precision	Recall	F-score	AUC	ρ_{\max}	Num. selected groups
GSVB-D	0.915 (0.013)	0.951 (0.011)	0.933 (0.009)	0.975 (0.004)	0.870 (0.016)	10
GSVB-B	0.916 (0.011)	0.958 (0.013)	0.936 (0.008)	0.975 (0.004)	0.875 (0.016)	12
SSGL	0.921 (0.012)	0.950 (0.011)	0.935 (0.009)	0.977 (0.004)	0.879 (0.015)	48
Group LASSO	0.924 (0.013)	0.952 (0.010)	0.938 (0.010)	0.977 (0.004)	0.882 (0.016)	60

Table 3: *Memset splice site detection*, evaluation metrics computed on the held out test data. Note that the test set was split into 10 folds and the mean (standard errors) of the metrics are computed.

6 Discussion

In this manuscript we have introduced GSVB, a scalable method for group sparse regression. We have shown how a fast co-ordinate ascent variational inference algorithms can be constructed and used to compute the variational posterior.

Through extensive numerical studies we have demonstrated that GSVB provides state-of-the-art performance, offering a computationally inexpensive substitute to MCMC, whilst also performing comparably or better than MAP methods. Additionally, through our analysis of real world datasets we have highlighted the practical utility of our method. Demonstrating, that GSVB provides parsimonious models with excellent predictive performance, and as demonstrated in Section 5.1, selects variables with established biological significance. Finally, different to MAP and frequentist methods, GSVB provides scalable uncertainty quantification, which serves as a powerful tool in several application areas.

There are several avenues for future work, for example extensions to other model families such as the multinomial, Gamma or negative Binomial. Other avenues, include extensions of the prior and variational families to different group structures, for example, when group are overlapping, or there is sparsity within groups. The later of which may would serve of particular importance when groups are large and effects within believed to be sparse.

SUPPLEMENTARY MATERIAL

R-package: R-package `gsvb` containing code to run our co-ordinate ascent variational inference algorithm presented in Algorithm 1. The package is available at <https://github.com/mkomod/gsvb>.

R scripts and data for numerical study and real world data analysis: these are used to produce the results reported in the paper, available at <https://github.com/mkomod/p3>.

References

- S. D. Babacan, S. Nakajima, and M. N. Do. Bayesian group-sparse modeling and variational inference. *IEEE Transactions on Signal Processing*, 62(11):2906–2921, 2014. ISSN 1053587X. doi: 10.1109/TSP.2014.2319775.
- R. Bai, G. E. Moran, J. L. Antonelli, Y. Chen, and M. R. Boland. Spike-and-Slab Group Lassos for Grouped Regression and Sparse Generalized Additive Models. *Journal of the American Statistical Association*, 0(0):1–41, 2020. ISSN 1537274X. doi: 10.1080/01621459.2020.1765784. URL <https://doi.org/10.1080/01621459.2020.1765784>.
- J. A. Blake, R. Baldarelli, J. A. Kadin, J. E. Richardson, C. L. Smith, and C. J. Bult. Mouse Genome Database (MGD): Knowledgebase for mouse-human comparative biology. *Nucleic Acids Research*, 49(D1):D981–D987, 2021. ISSN 13624962. doi: 10.1093/nar/gkaa1083.
- D. M. Blei, A. Kucukelbir, and J. D. McAuliffe. Variational Inference: A Review for Statisticians. *Journal of the American Statistical Association*, 112(518):859–877, 2017. ISSN 1537274X. doi: 10.1080/01621459.2017.1285773.
- P. Breheny and J. Huang. Penalized methods for bi-level variable selection. *Statistics and Its Interface*, 2(3):369–380, 2009. ISSN 19387989. doi: 10.4310/sii.2009.v2.n3.a10.
- P. Breheny and J. Huang. Group descent algorithms for nonconvex penalized linear and logistic regression models with grouped predictors. *Statistics and Computing*, 25(2):173–187, mar 2015. ISSN 0960-3174. doi: 10.1007/s11222-013-9424-2. URL <http://link.springer.com/10.1007/s11222-013-9424-2>.
- C. Burge and S. Karlin. Prediction of complete gene structures in human genomic DNA11Edited by F. E. Cohen. *Journal of Molecular Biology*, 268(1):78–94, 1997. URL <http://www.sciencedirect.com/science/article/pii/S0022283697909517>.

- P. Carbonetto and M. Stephens. Scalable variational inference for bayesian variable selection in regression, and its accuracy in genetic association studies. *Bayesian Analysis*, 7(1):73–108, 2012. ISSN 19360975. doi: 10.1214/12-BA703.
- R. B. Chen, C. H. Chu, S. Yuan, and Y. N. Wu. Bayesian Sparse Group Selection. *Journal of Computational and Graphical Statistics*, 25(3):665–683, 2016. ISSN 15372715. doi: 10.1080/10618600.2015.1041636.
- H. Chipman. Bayesian variable selection with related predictors. *Canadian Journal of Statistics*, 24(1):17–36, 1996. ISSN 03195724. doi: 10.2307/3315687.
- N. Depraetere and M. Vandebroek. A comparison of variational approximations for fast inference in mixed logit models. *Computational Statistics*, 32(1):93–125, 2017. ISSN 16139658. doi: 10.1007/s00180-015-0638-y.
- J. Huang and T. Zhang. The benefit of group sparsity. *Annals of Statistics*, 38(4):1978–2004, 2010. ISSN 00905364. doi: 10.1214/09-AOS778.
- J. Huang, S. Ma, H. Xie, and C. H. Zhang. A group bridge approach for variable selection. *Biometrika*, 96(2):339–355, 2009. ISSN 00063444. doi: 10.1093/biomet/asp020.
- J. Huang, J. L. Horowitz, and F. Wei. Variable selection in nonparametric additive models. *Annals of Statistics*, 38(4):2282–2313, 2010. ISSN 00905364. doi: 10.1214/09-AOS781.
- J. Huang, P. Breheny, and S. Ma. A selective review of group selection in high-dimensional models. *Statistical Science*, 27(4):481–499, 2012. ISSN 08834237. doi: 10.1214/12-STS392.
- T. S. Jaakkola and M. I. Jordan. A variational approach to Bayesian logistic regression models and their extensions, 1996.
- L. Jacob, G. Obozinski, and J. P. Vert. Group lasso with overlap and graph lasso. *ACM International Conference Proceeding Series*, 382, 2009. doi: 10.1145/1553374.1553431.
- R. Jreich, C. Hatte, and E. Parent. Review of Bayesian selection methods for categorical predictors using JAGS. *Journal of Applied Statistics*, 49(9):2370–2388, 2022. ISSN 13600532. doi: 10.1080/02664763.2021.1902955. URL <https://doi.org/10.1080/02664763.2021.1902955>.

- M. Komodromos, E. O. Aboagye, M. Evangelou, S. Filippi, and K. Ray. Variational Bayes for high-dimensional proportional hazards models with applications within gene expression. *Bioinformatics*, 38(16):3918–3926, aug 2022. ISSN 1367-4803. doi: 10.1093/bioinformatics/btac416. URL <https://academic.oup.com/bioinformatics/article/38/16/3918/6617825>.
- M. Kyung, J. Gilly, M. Ghoshz, and G. Casellax. Penalized regression, standard errors, and Bayesian lassos. *Bayesian Analysis*, 5(2):369–412, 2010. ISSN 19360975. doi: 10.1214/10-BA607.
- W. T. Lai and R. B. Chen. A review of Bayesian group selection approaches for linear regression models. *Wiley Interdisciplinary Reviews: Computational Statistics*, 13(4): 1–22, 2021. ISSN 19390068. doi: 10.1002/wics.1513.
- K. Lee and X. Cao. Bayesian group selection in logistic regression with application to MRI data analysis. *Biometrics*, 77(2):391–400, 2021. ISSN 15410420. doi: 10.1111/biom.13290.
- K. Lounici, M. Pontil, S. Van De Geer, and A. B. Tsybakov. Oracle inequalities and optimal inference under group sparsity. *Annals of Statistics*, 39(4):2164–2204, 2011. ISSN 00905364. doi: 10.1214/11-AOS896.
- M. Matsui, F. Sakurai, S. Elbashir, D. J. Foster, M. Manoharan, and D. R. Corey. Activation of LDL Receptor Expression by Small RNAs Complementary to a Non-coding Transcript that Overlaps the LDLR Promoter. *Chemistry & Biology*, 17(12): 1344–1355, dec 2010. ISSN 10745521. doi: 10.1016/j.chembiol.2010.10.009. URL <https://linkinghub.elsevier.com/retrieve/pii/S1074552110004023>.
- L. Meier, S. Van De Geer, and P. Bühlmann. The group lasso for logistic regression. *Journal of the Royal Statistical Society. Series B: Statistical Methodology*, 70(1):53–71, 2008. ISSN 13697412. doi: 10.1111/j.1467-9868.2007.00627.x.
- T. J. Mitchell and J. J. Beauchamp. Bayesian variable selection in linear regression. *Journal of the American Statistical Association*, 83(404):1023–1032, 1988. ISSN 1537274X. doi: 10.1080/01621459.1988.10478694.

- K. P. Murphy. Conjugate bayesian analysis of the gaussian distribution, 2007. URL <https://www.cs.ubc.ca/~murphyk/Papers/bayesGauss.pdf>.
- M. Opper and C. Archambeau. The variational gaussian approximation revisited. *Neural Computation*, 21(3):786–792, 03 2009. ISSN 0899-7667. doi: 10.1162/neco.2008.08-07-592. URL <https://doi.org/10.1162/neco.2008.08-07-592>.
- J. T. Ormerod, C. You, and S. Müller. A variational bayes approach to variable selection. *Electronic Journal of Statistics*, 11(2):3549–3594, 2017. ISSN 19357524. doi: 10.1214/17-EJS1332.
- S. Raman, T. J. Fuchs, P. J. Wild, E. Dahl, and V. Roth. The bayesian group-lasso for analyzing contingency tables. *ACM International Conference Proceeding Series*, 382: 881–888, 2009. doi: 10.1145/1553374.1553487.
- K. Ray, B. Szabo, and G. Clara. Spike and slab variational Bayes for high dimensional logistic regression. In H. Larochelle, M. Ranzato, R. Hadsell, M. F. Balcan, and H. Lin, editors, *Advances in Neural Information Processing Systems*, volume 33, pages 14423–14434. Curran Associates, Inc., 2020. URL <https://proceedings.neurips.cc/paper/2020/file/a5bad363fc47f424ddf5091c8471480a-Paper.pdf>.
- V. Ročková and E. I. George. The Spike-and-Slab LASSO. *Journal of the American Statistical Association*, 113(521):431–444, 2018. ISSN 1537274X. doi: 10.1080/01621459.2016.1260469. URL <https://doi.org/10.1080/01621459.2016.1260469>.
- T. E. Scheetz, K. Y. A. Kim, R. E. Swiderski, A. R. Philp, T. A. Braun, K. L. Knudtson, A. M. Dorrance, G. F. DiBona, J. Huang, T. L. Casavant, V. C. Sheffield, and E. M. Stone. Regulation of gene expression in the mammalian eye and its relevance to eye disease. *Proceedings of the National Academy of Sciences of the United States of America*, 103(39):14429–14434, 2006. ISSN 00278424. doi: 10.1073/pnas.0602562103.
- M. Seeger. Bayesian methods for support vector machines and Gaussian processes. Master’s thesis, University of Karlsruhe, 1999. URL <http://people.mmci.uni-saarland.de/~mseeger/papers/bayes-svm.pdf>.
- M. G. Silverman, B. A. Ference, K. Im, S. D. Wiviott, R. P. Giugliano, S. M. Grundy, E. Braunwald, and M. S. Sabatine. Association between lowering LDL-C and cardio-

- vascular risk reduction among different therapeutic interventions: A systematic review and meta-analysis. *JAMA - Journal of the American Medical Association*, 316(12):1289–1297, 2016. ISSN 15383598. doi: 10.1001/jama.2016.13985.
- N. Simon, J. Friedman, T. Hastie, and R. Tibshirani. A sparse-group lasso. *Journal of Computational and Graphical Statistics*, 22(2):231–245, 2013. ISSN 10618600. doi: 10.1080/10618600.2012.681250.
- L. Wang, G. Chen, and H. Li. Group SCAD regression analysis for microarray time course gene expression data. *Bioinformatics*, 23(12):1486–1494, 2007. ISSN 13674811. doi: 10.1093/bioinformatics/btm125.
- X. Xu and M. Ghosh. Bayesian variable selection and estimation for group lasso. *Bayesian Analysis*, 10(4):909–936, 2015. ISSN 19316690. doi: 10.1214/14-BA929.
- G. Yeo and C. B. Burge. Maximum entropy modeling of short sequence motifs with applications to RNA splicing signals. *Journal of Computational Biology*, 11(2-3):377–394, 2004. ISSN 10665277. doi: 10.1089/1066527041410418.
- M. Yuan and Y. Lin. Model selection and estimation in regression with grouped variables. *Journal of the Royal Statistical Society. Series B: Statistical Methodology*, 68(1):49–67, 2006. ISSN 13697412. doi: 10.1111/j.1467-9868.2005.00532.x.
- C. Zhang, J. Butepage, H. Kjellstrom, and S. Mandt. Advances in Variational Inference. *IEEE Transactions on Pattern Analysis and Machine Intelligence*, 41(8):2008–2026, 2019. ISSN 19393539. doi: 10.1109/TPAMI.2018.2889774.

SUPPLEMENTARY MATERIAL

A Co-ordinate ascent algorithms

Derivations are presented for the variational family \mathcal{Q}' , noting that $\mathcal{Q} \subset \mathcal{Q}'$, hence the update equations under \mathcal{Q} follow directly from those under \mathcal{Q}' . Recall, the family is given as,

$$\mathcal{Q}' = \left\{ Q'(\mu, \Sigma, \gamma) = \bigotimes_{k=1}^M Q'_k(\mu_{G_k}, \Sigma_{G_k}, \gamma_k) := \bigotimes_{k=1}^M [\gamma_k N(\mu_{G_k}, \Sigma_{G_k}) + (1 - \gamma_k)\delta_0] \right\} \quad (\text{A.1})$$

where $\Sigma \in \mathbb{R}^{p \times p}$ is a covariance matrix for which $\Sigma_{ij} = 0$, for $i \in G_k, j \in G_l, k \neq l$ (i.e. there is independence between groups) and $\Sigma_{G_k} = (\Sigma_{ij})_{i,j \in G_k} \in \mathbb{R}^{m_k \times m_k}$ denotes the covariance matrix of the k th group.

A.1 Gaussian Family

Under the Gaussian family, $Y_i \stackrel{\text{iid}}{\sim} N(x_i^\top \beta, \tau^2)$, and the log-likelihood is given by,

$$\ell(\mathcal{D}; \beta, \tau^2) = -\frac{n}{2} \log(2\pi\tau^2) - \frac{1}{2\tau^2} \|y - X\beta\|^2.$$

Recall, we have chosen to model τ^2 by an inverse-Gamma prior which has density,

$$\frac{b^a}{\Gamma(a)} x^{-a-1} \exp\left(\frac{-b}{x}\right)$$

where $a, b > 0$ and in turn we extend \mathcal{Q}' to $\mathcal{Q}'_\tau = \mathcal{Q}' \times \{\Gamma^{-1}(a', b') : a', b' > 0\}$.

Under this variational family, the expectation of the negative log-likelihood is given by,

$$\begin{aligned} \mathbb{E}_{Q'_\tau} [-\ell(\mathcal{D}; \beta)] &= \mathbb{E}_{Q'_\tau} \left[\frac{n}{2} \log(2\pi\tau^2) + \frac{1}{2\tau^2} \|y - X\beta\|^2 \right] \\ &= \mathbb{E}_{Q'_\tau} \left[\frac{n}{2} \log(2\pi\tau^2) + \frac{1}{2\tau^2} (\|y\|^2 + \|X\beta\|^2 - 2\langle y, X\beta \rangle) \right] \\ &= \frac{n}{2} (\log(2\pi) + \log(b') - \kappa(a')) \\ &\quad + \frac{a'}{2b'} \left(\|y\|^2 + \left(\sum_{i=1}^p \sum_{j=1}^p (X^\top X)_{ij} \mathbb{E}_{Q'_\tau} [\beta_i \beta_j] \right) - 2 \sum_{k=1}^M \gamma_k \langle y, X_{G_k} \mu_{G_k} \rangle \right) \end{aligned} \quad (\text{A.2})$$

where the expectation

$$\mathbb{E}_{Q'_\tau} [\beta_i \beta_j] = \begin{cases} \gamma_k (\Sigma_{ij} + \mu_i \mu_j) & i, j \in G_k \\ \gamma_k \gamma_h \mu_i \mu_j & i \in G_k, j \in G_h, h \neq k \end{cases}$$

A.2 Binomial Family Re-parameterization

To re-parametrization of Σ_{G_k} we follow the same process as in Section 3.2.1. Formally, we have,

$$\Sigma_{G_k} = (X_{G_k}^\top A_t X_{G_k} + wI)^{-1} \quad (\text{A.3})$$

where $w \in \mathbb{R}$ is the free parameter to be optimized and $A_t = \text{diag}(a(t_1), \dots, a(t_n))$. Notably, this result follows due to the quadratic nature of the bound employed. Meaning we are able to re-parameterize Σ_{G_k} .

B Derivation of Variational Posterior Predictive

To compute the variational posterior predictive distribution for the Binomial and Poisson model, we sample $\beta \sim \tilde{\Pi}$ and then sample $y^*|x^*, \mathcal{D}$ from the respective distribution with mean given by $f(x^{*\top} \beta)$ where $x^* \in \mathbb{R}^p$ and f is the link function. To sample from $\tilde{\Pi}$ we sample $z_k \stackrel{\text{ind}}{\sim} \text{Bernoulli}(\gamma_k)$ and then $\beta_{G_k} \stackrel{\text{ind}}{\sim} N(\mu_{G_k}, \Sigma_{G_k})$ if $z_k = 1$ otherwise we set $\beta_{G_k} = 0_{m_k}$.

For the Gaussian family we are able to simplify the process by integrating out the variance τ^2 . Following Murphy (2007), substituting $\xi = \tau^2$ and recalling the independence of τ^2 and β in our variational family, we have,

$$\begin{aligned} \tilde{p}(y^*|x^*, \mathcal{D}) &\propto \int_{\mathbb{R}^p} \int_{R^+} \xi^{-(a'+1/2)-1} \exp\left(-\frac{(y^* - x^{*\top} \beta)^2 + 2b'}{2\xi}\right) d\xi d\tilde{\Pi}(\beta) \\ &\propto \int_{\mathbb{R}^p} \left(\frac{(y^* - x^{*\top} \beta)^2}{2b'} + 1\right)^{-(a'+1/2)} d\tilde{\Pi}(\beta) \end{aligned}$$

Recognizing that the expression within the integral has the same functional form as a generalized t -distribution, whose density is denoted as $t(x; \mu, \sigma^2, \nu) = \Gamma((\nu+1)/2)/(\Gamma(\nu/2)\sqrt{\nu\pi}\sigma)(1+(x-\mu)^2/(\nu\sigma^2))^{-(\nu+1)/2}$, yields,

$$\tilde{p}(y^*|x^*, \mathcal{D}) = \int_{\mathbb{R}^p} t(y^*; x^{*\top} \beta, b'/a', 2a') d\tilde{\Pi}(\beta) \quad (\text{B.1})$$

As (B.1) is intractable we instead sample from $p(y^*|x^*, \mathcal{D})$, by

1. Sampling $\beta \sim \tilde{\Pi}$.
2. Sampling y^* from $Y^* = \mu + \sigma t_\nu$ where $\mu = x^{*\top} \beta$, $\sigma = \sqrt{b'/a'}$ and $\nu = 2a'$, where t_ν denotes a t -distribution with ν degrees of freedom.

C Gibbs Sampler

We present a Gibbs sampler for the Gaussian family of models, noting that the samplers for the Binomial and Poisson family use the same principles. We begin by considering a slight alteration of the prior given in (2). Formally,

$$\begin{aligned}\beta_{G_k} &\stackrel{\text{iid}}{\sim} \Psi(\beta_{G_k}; \lambda) \\ z_k | \theta_k &\stackrel{\text{iid}}{\sim} \text{Bernoulli}(\theta_k) \\ \theta_k &\stackrel{\text{iid}}{\sim} \text{Beta}(a_0, b_0)\end{aligned}\tag{C.1}$$

for $k = 1, \dots, M$ and $\tau^2 = \xi \stackrel{\text{iid}}{\sim} \Gamma^{-1}(\xi; a, b)$. Under this prior writing the likelihood as,

$$p(\mathcal{D} | \beta, z, \xi) = \prod_{i=1}^n \phi\left(y_i; f\left(\sum_{k=1}^M z_k \langle x_{G_k}, \beta_{G_k} \rangle\right), \xi\right)\tag{C.2}$$

where $\phi(\cdot; \mu, \sigma^2)$ is the density of the Normal distribution with mean μ and variance σ^2 , and f is the link function (which in this case is the identity), yields the posterior

$$p(\beta, z, \xi | \mathcal{D}) \propto p(\mathcal{D} | \beta, z, \xi) \pi(\xi) \prod_{k=1}^M \pi(\beta_{G_k}) \pi(z_k | \theta_k) \pi(\theta_k).\tag{C.3}$$

Notably, the posterior is equivalent to our previous formulation.

To sample from (C.3), we construct a Gibbs sampler as outlined in Algorithm 2. Ignoring the superscript for clarity, the distribution $\theta_k | \mathcal{D}, \beta, z, \theta_{-k}, \xi$ is conditionally independent of $\mathcal{D}, \beta, z_{-k}, \xi$ and θ_{-k} . Therefore, θ_k is sampled from $\theta_k | z_k$, which has a $\text{Beta}(a_0 + z_k, b_0 + 1 - z_k)$ distribution. Regarding $z_j^{(i)}$, the conditional density

$$\begin{aligned}p(z_k | \mathcal{D}, \beta, z_{-k}, \theta, \xi) &\propto p(\mathcal{D} | \beta, z_{-k}, z_k, \theta, \xi) \pi(z_k | \beta, z_{-k}, \theta, \xi) \\ &= p(\mathcal{D}; \beta, z, \xi) \pi(z_k | \theta_k).\end{aligned}\tag{C.4}$$

As z_k is discrete, evaluating the RHS of (C.4) for $z_k = 0$ and $z_k = 1$, gives the unnormalised conditional probabilities. Summing gives the normalisation constant and thus we can sample z_k from a Bernoulli distribution with parameter

$$p_k = \frac{p(z_k = 1 | \mathcal{D}, \beta, z_{-k}, \theta, \xi)}{p(z_k = 0 | \mathcal{D}, \beta, z_{-k}, \theta, \xi) + p(z_k = 1 | \mathcal{D}, \beta, z_{-k}, \theta, \xi)}.\tag{C.5}$$

Finally, regarding $\beta_{G_{k,j}}^{(i)}$ we use a Metropolis-Hastings within Gibbs step, wherein a proposal $\beta_{G_{k,j}}^{(i)}$ is sampled from a random-walk proposition kernel K , where in our implementation

$K(x|\vartheta, \varepsilon) = N(x; \vartheta, \sqrt{2}(10^{1-\varepsilon})^{1/2})$. The proposal is then accepted with probability A or rejected with probability $1 - A$, in which case $\beta_{G_k,j}^{(i)} \leftarrow \beta_{G_k,j}^{(i-1)}$, where A is given by,

$$A = \min \left(1, \frac{p(\mathcal{D}; \beta_{G_k}^c, \beta_{G_k,-j}, \beta_{G_k,j}^{(i)}, z, \xi) \pi(\beta_{G_k,j}^{(i)} | \beta_{G_k,-j})}{p(\mathcal{D}; \beta_{G_k}^c, \beta_{G_k,-j}, \beta_{G_k,j}^{(i-1)}, z, \xi) \pi(\beta_{G_k,j}^{(i-1)} | \beta_{G_k,-j})} \frac{K(\beta_j^{(i-1)} | \beta_j^{(i)}, z_k^{(i)})}{K(\beta_j^{(i)} | \beta_j^{(i-1)}, z_k^{(i-1)})} \right)$$

Algorithm 2 MCMC sampler for the Gaussian family GSpSL regression

Initialize $\beta^{(0)}, z^{(0)}, \theta^{(0)}, \xi^{(0)}$

for $i = 1, \dots, N$

for $k = 1, \dots, M$

$\theta_k^{(i)} \stackrel{\text{iid.}}{\sim} \text{Beta}(a_0 + z_k^{(i-1)}, b_0 + 1 - z_k^{(i-1)})$

for $k = 1, \dots, M$

$z_k^{(i)} \stackrel{\text{ind.}}{\sim} \text{Bernoulli}(p_k)$

for $k = 1, \dots, M$

for $j = 1, \dots, m_k$

$\beta_{G_k,j}^{(i)} \sim p(\beta_{G_k,j}^{(i)} | \mathcal{D}, z^{(i)}, \beta_{G_{1:k-1}}^{(i)}, \beta_{G_{k,1:j-1}}^{(i)}, \beta_{G_{k,j+1:m_k}}^{(i-1)}, \beta_{G_{k+1:M}}^{(i-1)}, \xi^{(i-1)})$

 Sample $\xi^{(i)} \stackrel{\text{iid.}}{\sim} \Gamma^{-1}(a + 0.5n, b + 0.5\|y - \sum_{k=1}^M z_k X_{G_k} \beta_{G_k}^{(i)}\|^2)$

return $\{\beta^{(i)}, z^{(i)}, \theta^{(i)}, \xi^{(i)}\}_{i=1}^N$.

D Numerical Study

D.1 Performance with large groups

The performance of GSVB with large groups is examined. For this we fix $(n, p, s) = (1,000, 5,000, 10)$ and vary the group size to be $m = 10, 20, 25, 50, 100$. The results, presented in Figure 5 highlight that the performance of the method is excellent for groups of size $m = 10, 20, 25$, and begins to suffer when groups are of size $m = 50$ and 100 , particularly in settings 3 and 4 wherein GSVB-B did not run.

D.2 Runtime

Runtimes for the experiments presented in Section 4 are presented in Table 4 and Table 5. Notably, the runtime for GSVB over MCMC is orders of magnitudes faster. The runtime

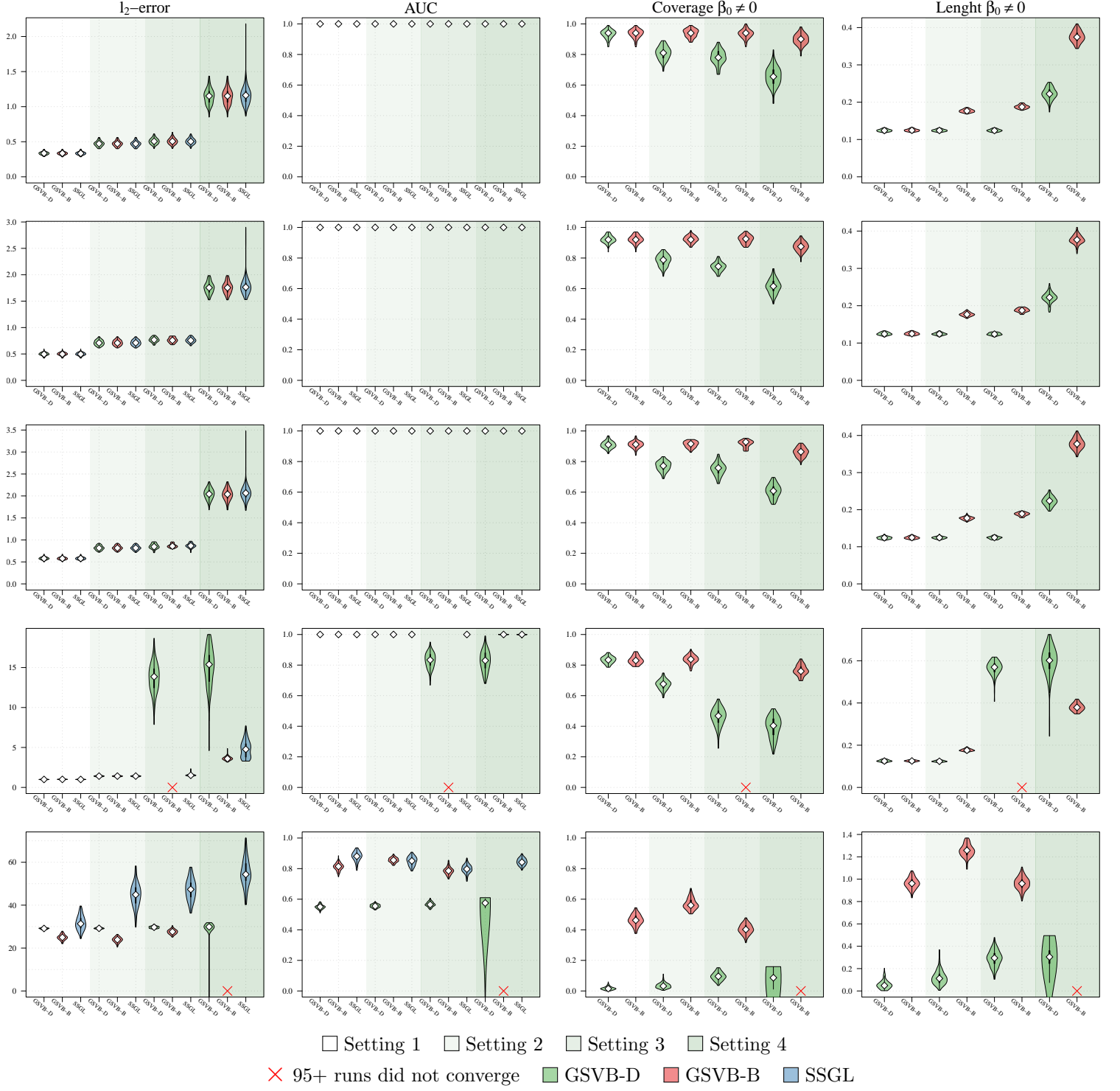


Figure 5: Performance evaluation of GSVB and SSSL for Settings 1–4 with $(n, p, s) = (1,000, 5,000, 10)$ across 100 runs. For each method the white diamond (\diamond) indicates the median of the metric, the thick black line (—) the interquartile range, and the black line (—) 1.5 times the interquartile range. **Rows 1–5:** Gaussian family with increasing group sizes of $m = 10, 20, 25, 50, 100$.

of GSVB in comparison to SSGL is slower in Settings 4, but marginally slower in the remaining settings. Note all simulations were ran on AMD EPYC 7742 CPUs (128 core, 1TB RAM).

	Method	Setting 1	Setting 2	Setting 3	Setting 4
Gaus. s=5	GSVB-D	2.1s (1.6s, 3.0s)	1.8s (1.1s, 2.9s)	3.5s (1.6s, 8.0s)	2.2s (1.6s, 5.2s)
	GSVB-B	1.8s (1.2s, 2.9s)	2.0s (1.3s, 3.1s)	3.4s (1.7s, 7.3s)	2.6s (1.8s, 6.7s)
	MCMC	7m 53s (7m 31s, 8m 12s)	7m 55s (7m 34s, 8m 2s)	7m 44s (7m 20s, 7m 48s)	8m 14s (7m 49s, 8m 17s)
Gaus. s=10	GSVB-D	2.3s (1.7s, 3.8s)	2.6s (1.9s, 3.9s)	7.4s (2.9s, 9.7s)	4.2s (2.4s, 12.1s)
	GSVB-B	2.9s (1.8s, 4.5s)	2.6s (2.2s, 3.2s)	9.5s (4.8s, 13.9s)	4.3s (2.7s, 14.0s)
	MCMC	9m 55s (9m 45s, 10m 8s)	10m 13s (9m 48s, 10m 30s)	9m 19s (9m 24s, 9m 33s)	10m 11s (9m 46s, 10m 27s)
Binom. s=3	GSVB-D	-	5.5s (3.5s, 9.3s)	7.7s (3.7s, 12.0s)	5.2s (2.7s, 8.0s)
	GSVB-B	-	7.2s (6.0s, 11.9s)	7.8s (5.6s, 14.4s)	6.0s (3.7s, 9.5s)
	MCMC	-	16m 45s (16m, 17m 15s)	16m 45s (15m 45s, 17m)	15m 45s (14m 49s, 16m 30s)
Pois. s=2	GSVB-D	3.6s (3.3s, 4.1s)	3.3s (2.9s, 3.7s)	3.1s (2.9s, 5.2s)	3.4s (2.4s, 4.1s)
	GSVB-B	12.5s (10.0s, 18.0s)	10.1s (7.9s, 14.5s)	15.5s (10.1s, 41.6s)	13.3s (10.5s, 24.0s)
	MCMC	15m 45s (14m 49s, 16m 45s)	15m 45s (15m 15s, 16m 30s)	16m (14m 59s, 18m)	18m 30s (16m 45s, 19m 45s)

Table 4: Median (5%, 95% quartile) runtimes for numerical experiments presented in Figure 1. Note $(n, p) = (200, 1000)$ for the Gaussian family and $(n, p) = (400, 1000)$ for the Binomial and Poisson family. Note that under setting 1 for the Binomial family there is perfect separation.

	Method	Setting 1	Setting 2	Setting 3	Setting 4
Gaus. m=10, s=10	GSVB-D	59.1s (47.2s, 1m 16s)	54.3s (47.5s, 1m 8s)	2m 53s (1m 4s, 6m 35s)	8m 7s (4m 30s, 25m 36s)
	GSVB-B	57.7s (50.7s, 1m 18s)	57.0s (49.5s, 1m 14s)	2m 51s (1m 7s, 6m 38s)	9m 45s (4m 53s, 25m 40s)
	SSGL	1m 3s (59.5s, 1m 13s)	50.8s (41.6s, 59.5s)	1m 1s (58.1s, 1m 16s)	1m 24s (1m 11s, 2m 3s)
Gaus. m=10, s=20	GSVB-D	3m 7s (3m 46s, 4m 31s)	3m 13s (3m 42s, 4m 39s)	9m 42s (3m 56s, 14m 54s)	20m 48s (6m 38s, 39m 23s)
	GSVB-B	3m 29s (3m 6s, 4m 20s)	3m 23s (3m 57s, 4m 48s)	12m 18s (4m 59s, 16m 20s)	34m 59s (12m 54s, 45m 2s)
	SSGL	2m 42s (1m 23s, 2m 3s)	1m 16s (59.2s, 2m 40s)	2m 6s (2m 37s, 2m 30s)	2m 16s (2m 31s, 6m 32s)
Binom. m=5, s=5	GSVB-D	-	3m 43s (2m 54s, 4m 54s)	2m 26s (2m 34s, 4m 5s)	2m 50s (1m 16s, 3m 30s)
	GSVB-B	-	4m 32s (3m 40s, 5m 8s)	3m 26s (2m 20s, 5m 26s)	2m 25s (2m 47s, 5m 18s)
	SSGL	-	2m 54s (2m 44s, 3m 42s)	3m 33s (2m 57s, 3m 26s)	2m 40s (2m 31s, 2m 3s)
Pois. m=5, s=3	GSVB-D	16.3s (9.8s, 21.5s)	11.2s (8.2s, 20.8s)	16.0s (10.4s, 43.0s)	12.9s (8.6s, 48.7s)
	GSVB-B	2m 26s (2m 59s, 3m 20s)	2m 55s (1m 29s, 3m 20s)	3m 53s (2m 49s, 9m 25s)	3m 33s (2m 4s, 9m 11s)
	SSGL	4m 11s (3m 49s, 8m 38s)	4m 34s (2m 11s, 13m 4s)	2m 29s (2m 56s, 16m 33s)	2m 32s (1m 25s, 3m 2s)

Table 5: Median (5%, 95% quartile) runtimes for numerical experiments presented in Figure 2. Note $(n, p) = (500, 5000)$ for the Gaussian family and $(n, p) = (1000, 5000)$ for the Binomial and Poisson family. Note that under setting 1 for the Binomial family there is perfect separation

E Real data analysis

E.1 Genetic determinants of LDL-C in mice

RSID (or probe ID)	Freq. GSVB-D	Freq. GSVB-B
rs13476279	6	6
rs13483823	6	5
CEL.4_130248229	5	3
rs13477968	3	5
rs13476241	4	3
CEL.X_65891570	2	4
rs13477903	2	2
rs3688710	2	1
rs13477939	1	-
rs3157124	1	-
rs13478204	-	3
rs6186902	-	2
rs13483814	-	1
rs4222922	-	1
rs6187266	-	1
UT_4_128.521481	-	1

Table 6: *Genetic determinants of LDL-C in mice*: SNPs selected by GSVB.

E.2 Bardet-Biedl Syndrome Gene Expression Study

Probe ID	Gene Name	Freq. GSVB-D	Freq. GSVB-B	Freq. SSGL
1383183_at		1	1	8
1386237_at		1	1	-
1397359_at		4	2	-
1386552_at		-	1	-
1378682_at		-	1	-
1385926_at		-	-	2
1396814_at		-	-	3
1386811_at	<i>Hacd4</i>	1	2	-
1386069_at	<i>Sp2</i>	4	2	-
1371209_at	<i>RT1-CE5</i>	-	1	-
1391624_at	<i>Sec14l3</i>	-	1	-
1383829_at	<i>Bbx</i>	-	2	-
1389274_at	<i>Dcakd</i>	-	-	1
1373995_at	<i>Abcg1</i>	-	-	1
1375361_at	<i>Snx18</i>	-	-	1
1368915_at	<i>Kmo</i>	-	-	7

Table 7: Bardet-Biedl syndrome gene expression study: variables selected by GSVB and SSGL.